Assessment of potentially toxic elements (PTEs) sources on soils surrounding a fossil fuel power plant in a semi-arid/arid environment: A case study from the Sonoran Desert

ReneéGonzález-Guzmán[a] ClaudioInguaggiato[ab] LorenzoBrusca[c] Zayre I.González-Acevedo[a] RubénBernard-Romero[a]

[a] Departamento de Geología, División de Ciencias de la Tierra, CICESE, Carretera Ensenada-Tijuana 3918, Zona Playitas, 22860 Ensenada, Baja California, Mexico

[b] Istituto Nazionale di Geofisica e Vulcanologia, Sezione di Bologna, Via Donato Creti 12, 40128 Bologna, Italy

[c] Istituto Nazionale di Geofisica e Vulcanologia, Sezione di Palermo, Via Ugo La Malfa, 153, Palermo, 90146, Italy

Editorial handling by Prof. M. Kersten

Highlights

- Topsoil around Puerto Libertad is influenced by natural and anthropogenic sources.
- The major oxides and REE in the soils are reliable genetic indicators of the bedrock.
- The anthropogenic source contributed to the accumulation of V, Ni, and Mo in the soils.
- The highest pollution markers in soils are found in the vicinity of the power plant.

Abstract

Understanding the sources of potentially toxic elements (PTEs) in soils is a worldwide challenge that requires effective discrimination between geogenic and anthropogenic contributions, particularly in areas with certain geological complexity. This study aims to examine the chemical contents of 23 topsoil samples collected from the surroundings of a fossil fuel power plant in the village of Puerto Libertad (Sonoran Desert, Mexico). The study did not exclusively focus on the source identification of the priority PTEs to evaluate soil pollution. Furthermore, major oxides and immobile trace element (Zr, Hf, and REE: La→Lu) data were provided for a reliable assessment of the provenance of the soils. The relatively high SiO_2 contents (65.26–75.42 wt%, anhydrous basis), the Post-Archean Australian Shale (PAAS)-normalized REE patterns, and the uniformity of the values of the Index of Compositional Variability (ICV = 1.11–2.72) and the Chemical Index of Alteration (CIA = 31.65–51.79) suggest that the soils were derived from intermediate to felsic source rocks, controlled by the

local weathering of the parent bedrocks, under a low degree of chemical weathering conditions. The PTE data were treated following a robust workflow, which included the use of the enrichment factor (EF), the Spearman rank correlation (ρ), and multivariate statistical analyses allowed the generation of significant elemental associations and the identification of pools related either to the geological background or to anthropogenic activities. The results suggesting that Mo and Zn concentrations present a moderate anthropogenic influence while the concentrations of Pb, Sn, Cu, Cd, As, Cr, and Co are predominantly of geogenic origin. Vanadium (avg. EFV = 3.4) and Ni (avg. EFNi = 4.6) were the most enriched elements in the soils. Moreover, the highest values of the integrated Nemerow Pollution Index (PI_N>3) were recorded at the sampling stations closer to the village, suggesting point-source pollution by the emissions of the power station. Finally, in this paper is traced the extent of the particulate released into the atmosphere, which can be dispersed in a wide area into the Sonoran Desert.

Graphical abstract

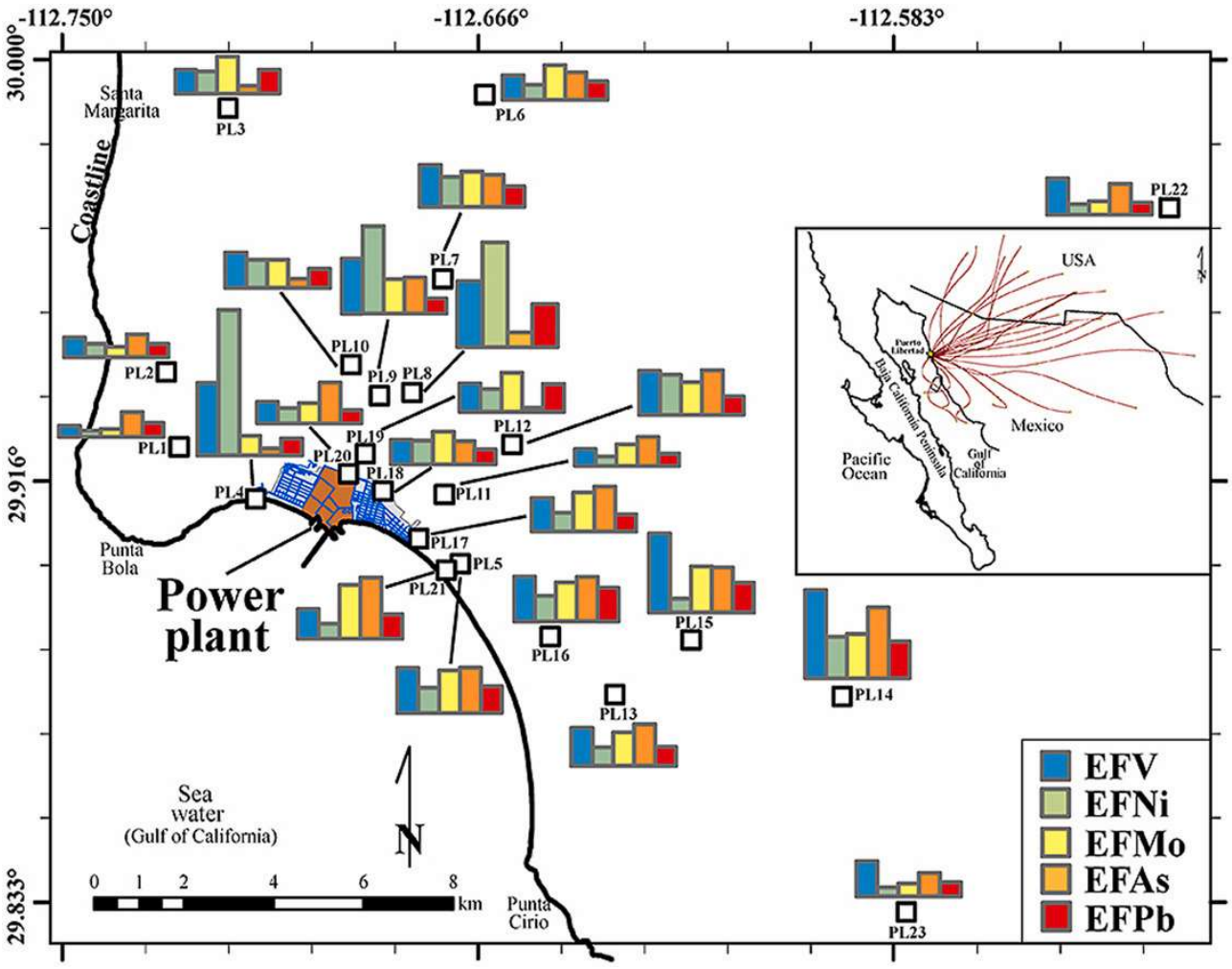

1. Introduction

Soil formation begins with the physical and chemical breakdown of continental Earth's rocks, caused by environmental agents (Amundson, 2014; Minasny et al., 2008). This process, known as weathering, chips away rock fragments into an array of smaller pieces and eventually into sand, silt,

and clay particles (Dorn, 2011; Jackson et al., 2002; Xia et al., 2015). Unlike chemical forms of weathering, physical processes are more pronounced in arid environments, transferring the mineralogical contents from bedrock to soils (Warke, 2013). In geochemical terms, several metals and metalloids, the so-called potentially toxic elements (PTEs) (Duffus, 2002; Pourret and Bollinger, 2018), occur naturally in amounts rarely toxic in the soil environment from pedogenetic processes of the weathering of parent materials at levels that are regarded as trace (<1000 mg kg−1) (Alloway, 2013; Cabral Pinto et al., 2017; Galán et al., 2014; Hooda, 2010; Mikkonen et al., 2018). Apart from this intrinsic nature, anthropogenic activities introduce the continuous low-level input of materials on topsoil and sediments from the deposition of atmospheric particulates (Christensen et al., 2018; Dinis et al., 2021; Gray et al., 2003; Prabhakar et al., 2014; Rueda-Holgado et al., 2016; Zheng et al., 2016). As a direct consequence, the enrichment of specific PTEs should be sensitive to a specific anthropogenic activity (Bosco et al., 2005; Cai et al., 2015; Franco-Uría et al., 2009; Heidari et al., 2021; Mikkonen et al., 2018; Rueda-Holgado et al., 2016; Tijhuis et al., 2002; Zheng et al., 2016). Particularly, the burn of fossil fuels emits residual oil fly ash (ROFA), which is characterized by a high content of contaminants (Al-Degs et al., 2014; Allouis et al., 2003; Boix et al., 2001; Häsänen et al., 1986; Moreno et al., 2010; Navarro et al., 2007). Several studies have concluded that PTEs such as V, Ni, Cr, and As multiply their concentration in sediments and soils in areas surrounding oil-fired power stations. Among these elements, V and Ni can be held as the most important elements for tracing the emissions of fuel combustion processes in power stations (Al-Ghouti et al., 2011; Al-Masri et al., 2015; Boix et al., 2001; Bosco et al., 2005; Meza-Montenegro et al., 2012; Pastrana-Corral et al., 2017).

In terms of PTE concentrations, soil quality has received considerable attention from the scientific community worldwide. In particular, soil pollution assessment is a concern for arid and semi-arid regions covering more than one-third of the global land area and supporting over a fifth of the world's population (Kebonye et al., 2017; Meza-Figueroa et al., 2007, 2018; Mukherjee et al., 2020; Prabhakar et al., 2014; Yang and Williams, 2015). Inherent physical factors that may greatly impact on the enrichment of PTEs in soils occur in this environment. For instance, arid and semi-arid backgrounds are characterized by a low amount of organic matter, scarce vegetation, poor soil structure, drought, heavy rainfalls during short rainy seasons, strong winds, and extreme temperatures and UV radiation (Khodaverdiloo et al., 2020; Moore and Carpi, 2005; Moreno-Rodríguez et al., 2015; Navarro et al., 2004, 2008; Ravankhah et al., 2017; Razo et al., 2004; Yang et al., 2017; Yang and Williams, 2015). Located in the Sonoran Desert, Puerto Libertad is an example of a semi-arid/arid area highly exposed to PTEs contamination from a practically unique local emission source. The village of Puerto Libertad hosts one of the biggest energy power plants of the Sonoran Desert, namely, Puerto Libertad Thermal Power Plant (PLTPP). The power plant is located in the geographic coordinates 29.9058 N and −112.6928 W. It began operations in 1985 and was designed as a conventional power station that involves the combustion of diesel, with a capacity of 632 MWe in its four units. Based only on data from 2002 to 2005 ("globalenergyobservatory," 2002–2005), the plant consumed 828 ktoe (thousand tonnes of oil equivalent) and emitted around 6158 tons of ROFA per year until 2017. According to the local literature, since 2017 the power plant has ceased to use heavy oil for electricity generation. Instead of this process, it changed to a combined cycle gas turbine (CCGT) technology. However, for more than 30 years, the power station has engaged in an open cycle of atmospheric particulate matter production and deposits that are directly connected to the soils around the village. The location of Puerto Libertad and the soil properties of the region make it an ideal area to assess PTEs enrichment and distinguish between the geological factors and the impact of the major anthropogenic activity on the environment. Such an impact can manifest itself in adverse effects on human health and the surrounding ecological system.

The present study investigates the geochemistry of topsoil in the Puerto Libertad area. The three scopes can be summarized as follows: (i) assess the potential bedrocks and weathering conditions of

the soils; (ii) identify the PTEs sources and distinguish between natural and anthropogenic influences with an emphasis on V and Ni (which are present in large amounts in the ROFA); (iii) constrain the main influence zone of the power plant installed in Puerto Libertad and the spatial patterns of the possible paths of the contaminants on a regional scale.

2. Materials and methods

2.1. Study area

In North America, an important region covered by an arid environment is the Sonoran Desert. It covers large portions of the southwestern United States and northwestern Mexico with more than 300,000 square kilometers (Fig. 1a). Their population was rapidly growing during the last decades and it houses large cities such as Phoenix and Tucson in Arizona, and Mexicali and Hermosillo in Mexico. Notwithstanding the concern of several workers to trace the anthropogenic source contributions in soils and sediments from urban, industrial, agricultural, and mining activities in the Sonoran Desert (e.g., Aguilar-Hinojosa et al., 2016; Calmus et al., 2018; García-Rico et al., 2016; González-Grijalva et al., 2019; Meza-Figueroa et al., 2007; Meza-Montenegro et al., 2012; Ochoa-Contreras et al., 2021; Prabhakar et al., 2014), there is a lack of information regarding the emission of pollutants from power stations (Fig. 1a).

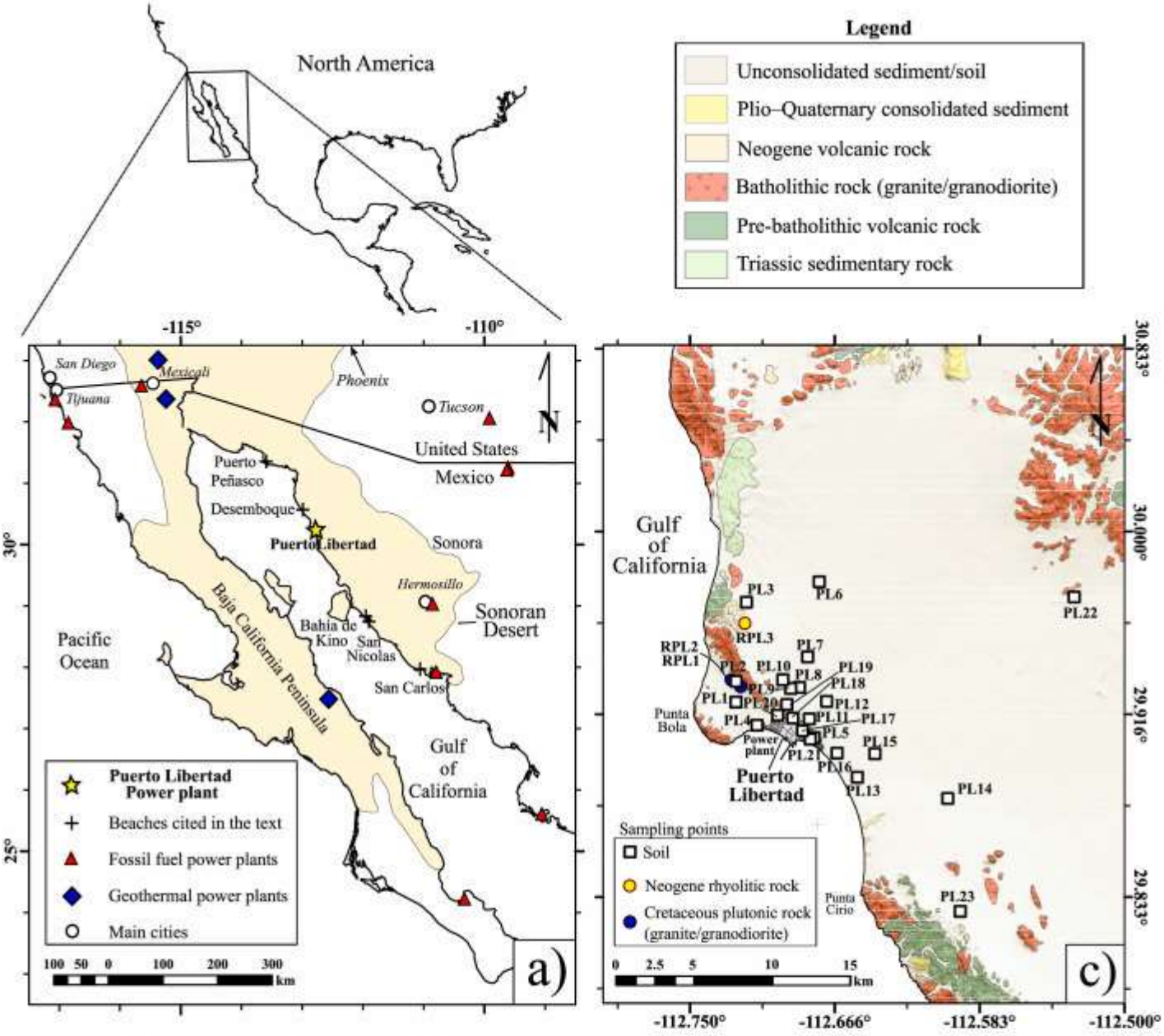
North America
Legend
Unconsolidated sediment/soil
Plio–Quaternary consolidated sediment
Neogene volcanic rock
Batholithic rock (granite/granodiorite)
Pre-batholithic volcanic rock
Triassic sedimentary rock
-115°
-110°
30°
25°
San Diego
Tijuana
Mexicali
Phoenix
Tucson
United States
Mexico
Puerto Peñasco
Desemboque
Puerto Libertad
Sonora
Hermosillo
Sonoran Desert
Bahia de Kino
San Nicolas
San Carlos
Baja California Peninsula
Pacific Ocean
Gulf of California
Puerto Libertad Power plant
Beaches cited in the text
Fossil fuel power plants
Geothermal power plants
Main cities
100 50 0 100 200 300 km
a)
Gulf of California
PL3
PL6
PL22
RPL3
RPL2
RPL1
PL7
PL2
PL10
PL8
PL19
PL9
PL18
PL1
PL20
PL12
Punta Bola
PL4
PL11
PL17
PL5
Power plant
PL15
PL2
PL16
Puerto Libertad
PL13
PL14
Sampling points
Soil
Neogene rhyolitic rock
Cretaceous plutonic rock (granite/granodiorite)
Punta Cirio
PL23
0 2.5 5 10 15 km
c)
30.833°
30.000°
29.916°
29.833°
-112.750°
-112.666°
-112.583°
-112.500°
1988
1998
2008
2018
N
W
E
S
40%
30%
20%
10%
mean = 4.1923
calm = 1.4%
mean = 3.6285
calm = 3%
mean = 2.9665
calm = 1.7%
mean = 3.9176
calm = 0%
b)
0 to 2
2 to 4
4 to 6
6 to 14
(m s-1)
Frequency of counts by wind direction (%)

Fig. 1. (a) Map showing the approximate boundaries of the Sonoran Desert (shaded area) in the southwestern United States and northwestern Mexico. In addition, the locations of the study area, beaches along the Sonoran coast, fossil fuel power plants, geothermal power plants, and main cities. (b) The wind roses indicate the dominant wind directions and the direction of the strongest wind speeds in the north of the Gulf of California. The period of record is between 1988 and 2018. Wind data are those reported by NOAA and plotted using the CRAN OpenAir (v.2.8.6) (Carslaw and Ropkins, 2012). (c) Geological map of the study area showing the locations of sampling sites (adopted from Gastil and Krummenacher, 1977). For the interpretation of the references to colors in the legend, the reader is referred to the web version of this paper. (For interpretation of the references to color in this figure legend, the reader is referred to the Web version of this article.)

The power station located in the research area is one of the biggest plants in northwestern Mexico but the hosted village, Puerto Libertad, is a small locality with approximately 2750 inhabitants (INEGI, 2020). Puerto Libertad is sited on the seashore of the Gulf of California, far from any major highway system or a big city (Fig. 1a). In addition, local mining and agro-industrial activities practically can be neglected; thus, the emissions produced during the fossil fuel combustion of the PLTPP are the main source of pollution in the Puerto Libertad area. The overall wind patterns throughout the region show that the prevailing wind flows are from moist ocean areas to dryland areas (Fig. 1b). In this sense, Puerto Libertad is on the circulation pattern typically developed by the North American Monsoon in late May or early June over Sonora (Adams and Comrie, 1997). Nonetheless, there is a local excess of evaporation over precipitation.

From the geological viewpoint, the area of Puerto Libertad is in the core of the Coastal Sonora Batholith (CSB, Valencia-Moreno et al., 2011). The area is tectonically affected by the late Cenozoic southern Basin and Range extensional province, characterized by numerous NNW–SSE-oriented and well-exposed basins (Henry, 1989). For its part, Gastil and Krummenacher (1977) described the local geology. The outcrop rocks in the area mainly comprise Laramidic granitic rocks (late Cretaceous) that are intruded into the volcanic and volcanoclastic strata of the early Cretaceous age. Furthermore, exhumed intermediate to felsic Neogene volcanic rocks occur in the north of Puerto Libertad (Fig. 1c). Generally, the geomorphic structure is a typical mountain-basin-coast system, in which marine and fluvial terrace deposits dominate the area. The coastal deposits are generally stable and well developed (Ortlieb, 1991). Along the Sonoran coast, the sand-sized deposits are predominantly eroded from granitoids from nearby outcrops (Armstrong-Altrin, 2009; Armstrong-Altrin et al., 2014; Madhavaraju et al., 2016; Ortega et al., 2013).

2.2. Sampling

Twenty-three topsoil samples were collected randomly from divergent sites around the PLTPP in April 2018. The upper ~0–10 cm soil were collected using a silicone spatula. The samples were collected until this depth in order to examine the part of the soil in which the effect of atmospheric particulate would have the strongest influence. The sites were also codified from PL1 to PL23. About 1.0 kg of each sample was placed in a resealable plastic bag and transported to the laboratory. In addition, the collection of rock samples was conducted upon the determination of the local background levels of the PTEs. Two rock samples belonging to a pluton of the CSB, namely, RPL1 and RPL2, and another of the rhyolitic composition (RPL3) collected nearly 8 km north of the PLTPP represent the bedrock in this study. The positions of the sampling points were recorded by a GPS instrument (Fig. 1c), and the information was implemented in a geographic information system (ArcGIS® 10.7, using WGS84 datum).

2.3. Analytical methods

Sample preparation and chemical procedures were performed using the SLE facilities at Divisón de Ciencias de la Tierra, CICESE, Mexico. An analysis with a stereo microscope was conducted to identify the mineral constituents of the soil samples. In addition, they were analyzed for pH, organic matter (OM) content, and particle sizes. The pH was determined by a portable pH meter (Thermo-Scientific® Orion Star® brand) in a 1:2.5 solution (sample: deionized water [resistivity 18.2 Ω cm^{-1}]). The OM was also determined by titration through oxidation by dichromate in an acidic medium (Gaudette et al., 1974). Granulometric analysis was executed by employing the gravimetric method to determine the size of the distinct particles in soils. Additionally, the bulk material was passed through a sample splitter to obtain a representative aliquot of each soil sample. Approximately 100 g of such an aliquot was powdered in an agate mill for chemical analysis. The major oxide compositions of the soils were obtained by X-ray fluorescence in fused $LiBO_2/Li_2B_4O_7$ disks using a Bruker® S8 Tiger ECO with an Rh-anode X-ray tube as a radiation source. The relative uncertainties were better than ±2%. An aliquot of all the samples were digested in a fresh mixture of the ultra-pure grade of HF (28 M), HNO_3 (16 M), and HCl (6 M) acids, in a volume ratio of 1:1:3, to ensure the complete dissolution of soil components. The compositions of V, Cr, Co, Ni, Rb, Cu, Zn, As, Mo, Cd, Sn, Sb, Pb, Zr, Hf and the fourteen lanthanoids were determined in solution by an Agilent® 7500ce inductively coupled plasma mass spectrometer (ICP-MS) at INGV, Palermo, Italy. Both accuracy and precision of the measurement were better than ±10%. Furthermore, whole-rock geochemical analysis was carried out by a quadrupole ICP-MS (Thermo Scientific® Q-ICP-MS) housed at LEI, UNAM. The results of major and trace elements of several international standards analyzed in the same batches were compared with certified values to check the quality and accuracy of the analyses (Table 1S, 2S, and 3S). The supplementary material presents further details of the analytical methods.

2.4. Data analysis

The major element data (Table 4S) were recalculated on an anhydrous basis and adjusted to 100% before using them in various indices and graphics. The Chemical Index of Alteration (CIA) (Nesbitt and Young, 1982), and the Index of Compositional Variability (ICV) (Cox et al., 1995) were used to interpret the degree of chemical weathering and to trace the source rocks and provenance of the soils. For the elimination of the complexities of the Oddo-Harkins effect and for the calculation of Eu-anomalies, REEs were normalized to the Post-Archean Australian Shale (PAAS) values after McLennan (1989).

Some basic statistical parameters of the PTEs**,** such as mean, standard deviation, extreme values (min and max), and skewness, were calculated (Table 5S). Spearman's (non-parametric) rank-order correlation analysis was performed to identify the relationship among PTEs, Zr, and OM. Results with $p < .05$ were considered statistically significant. On the other hand, principal component analysis (PCA) was applied to the data set to identify the underlying structure and provide an overview of the distribution pattern of those variables. These analyses were conducted with R (v. 3.6.3;R, 2020), a free software environment for statistical computing and graphics. The anthropogenic impacts of the soils were determined through two parameters. (i) The enrichment factor (EF; Buat-Menard and Chesselet, 1979) of individual PTEs was calculated to understand the contribution of geogenic and anthropogenic sources. The compositions of local rocks were used as backgrounds, and Ti was employed as a reference element for the EF calculation due to the natural association with trace elements in the bedrocks and relatively low mobility in weathering environments (Bern et al., 2011; Calmus et al., 2018). (ii) A quantitative measure of the extent of the overall PTEs pollution in the studied soils was calculated using the integrated Nemerow Pollution Index (PI_N; Weissmannová and Pavlovský, 2017). The geogenic background was identified on the basis of the abundance of the trace elements of the parent material, specifically the REE-normalized patterns of the local rocks, to obtain a more realistic assessment. The degree of enrichment (EF) or pollution (PI_N) of the soils are classified

according to the categories summarized in Weissmannová and Pavlovský (2017). The supplementary material displays further details of the data analysis.

2.5. Air forward trajectories analysis

The Global Data Assimilation System (GDAS 1.0) dataset from Air Resources Laboratory (ARL, NOAA) was used to drive Hybrid Single-Particle Lagrangian Integrated Trajectory (HYSPLIT) models using OpenAir (v.2.8.6, R environment) (Carslaw and Ropkins, 2012). Such models calculated forward air parcel trajectories starting daily at 00:00, 06:00, 12:00, and 18:00 (UTC) from Puerto Libertad for six days in 2015. The starting height for trajectory calculations was 100 m above sea level, and each trajectory was tracked for 24 h. That way, our computed trajectories represent the potential atmospheric transport routes of the ROFA from the PLPP.

3. Results

3.1. Physicochemical parameters

Table 1 exhibits the geographic coordinates, particle size fractions, pH, and OM contents of the soil samples from Puerto Libertad. The soils are formed mainly by unconsolidated parent materials (Fig. 1S). The mineral fraction is predominantly composed of quartz, feldspars, and phyllosilicates, and no calcium carbonate ($CaCO_3$) content in the samples is found. The grain-size percentage composition budget is dominated by sand (from 77.42% to 97.44%) at all sites (Fig. 2S). The OM contents are in the range of 0.30%–4.15% and presents significant correlations vs. V ($\rho = 0.63$; $p = .002$) and Ni ($\rho = 0.58$; $p = .004$). All soils are in the pH range from 8.27 to 9.27 (alkaline conditions).

Table 1. Locations, percentage grain-size distribution, percentage of organic matter, and pH of Puerto Libertad soil samples.

ID	Coordinates		[a]Distance (km)	Grain-size distribution (%)			Type	Organic matter(%)	pH
	Longitude	Latitude		Sand	Silt	Clay			
PL1	−112.72663	29.92346	4.59	97.44%	2.13%	0.43%	Poorly Sorted Very Coarse Sand	0.46	8.63
PL2	−112.72647	29.93869	5.42	95.28%	3.92%	0.80%	Poorly Sorted Very Coarse Sand	0.53	8.96
PL3	−112.71680	29.99056	9.66	85.41%	12.16%	2.40%	Very Coarse Silty Very Coarse Sand	1.56	8.62
PL4	−112.71022	29.91293	2.49	90.29%	8.09%	1.60%	Fine Silty Fine Sand	1.63	8.73
PL5	−112.67296	29.89916	1.99	92.74%	6.05%	1.20%	Very Coarse Silty Medium Sand	1.38	8.42
PL6	−112.66537	29.99315	9.76	84.39%	12.18%	3.44%	Poorly Sorted Very Coarse Sand	0.77	8.58

ID	Coordinates		[a]Distance (km)	Grain-size distribution (%)			Type	Organic matter(%)	pH
	Longitude	Latitude		Sand	Silt	Clay			
PL7	−112.67377	29.95665	5.60	91.34%	7.22%	1.40%	Fine Silty Fine Sand	1.71	8.27
PL8	−112.67993	29.93425	3.01	83.88%	13.43%	2.70%	Poorly Sorted Very Coarse Sand	2.24	8.57
PL9	−112.68643	29.93355	2.80	92.55%	6.21%	1.20%	Very Coarse Silty Very Coarse Sand	3.40	8.70
PL10	−112.69213	29.93978	3.51	77.42%	18.82%	3.76%	Poorly Sorted Coarse Sand	3.27	8.76
PL11	−112.67339	29.91402	1.77	93.44%	5.46%	1.10%	Poorly Sorted Very Coarse Sand	0.81	9.19
PL12	−112.65978	29.92392	3.60	94.32%	4.77%	0.90%	Poorly Sorted Coarse Sand	1.75	8.62
PL13	−112.63923	29.87443	6.64	93.95%	5.04%	1.00%	Poorly Sorted Fine Sand	0.91	8.76
PL14	−112.59366	29.87406	11.20	89.85%	8.46%	1.70%	Medium Silty Very Coarse Sand	1.02	8.52
PL15	−112.62399	29.88529	2.21	95.38%	3.85%	0.77%	Poorly Sorted Medium Sand	0.30	8.40
PL16	−112.65225	29.88595	2.01	91.20%	7.33%	1.50%	Poorly Sorted Very Fine Sand	2.11	8.91
PL17	−112.67868	29.90537	1.13	94.20%	4.83%	1.00%	Poorly Sorted Fine Sand	0.78	8.45
PL18	−112.68587	29.91477	0.74	91.93%	6.73%	1.30%	Poorly Sorted Very Coarse Sand	1.05	8.32
PL19	−112.69029	29.91687	0.95	95.16%	4.03%	0.80%	Poorly Sorted Very Coarse Sand	0.58	9.02
PL20	−112.69262	29.91806	1.16	89.77%	8.52%	1.70%	Very Coarse Silty Very Coarse Sand	1.20	9.13
PL21	−112.67021	29.90038	2.21	94.08%	4.93%	0.99%	Poorly Sorted Very Coarse Sand	0.70	9.27
PL22	−112.52816	29.97091	19.13	84.39%	12.17%	3.44%	Poorly Sorted Very Coarse Sand	4.15	8.55

ID	Coordinates		[a]Distance (km)	Grain-size distribution (%)			Type	Organic matter(%)	pH
	Longitude	Latitude		Sand	Silt	Clay			
PL23	−112.58604	29.82457	14.74	93.86%	5.11%	1.00%	Poorly Sorted Very Coarse Sand	1.54	8.58

a

Distance from the power station to the sampling point.

3.2. Major and trace element concentrations in soils

Table 4S presents the major and selected trace element contents of the soils from Puerto Libertad. Silica ranging between 65.26 and 75.42 wt% and Al_2O_3 contents varying from 11.44 to 15.46 wt%, indicate a felsic source essentially. The concentrations of Na_2O (2.70–4.46 wt%) and K_2O (2.70–4.68 wt%) are relatively homogeneous whereas large variations are observed in TiO_2 (0.19–0.60 wt%), Fe_2O_3 (1.43–7.18 wt%), MnO (0.02–0.06 wt%), MgO (0.33–2.19 wt%), CaO (0.46–8.10 wt%), and P_2O (0.03–0.21 wt%). All the major oxide data (wt.%) are recalculated on an anhydrous basis.

Conservative trace element contents are assessed to provide insight into the geochemical provenance of the soils. They are largely inherited from the parent rocks, as is indicated by the relatively high variation in the concentrations of the high field strength elements (HFSEs), such as Zr (23.44–141.53 ppm) and Hf (0.82–3.55 ppm). Total REE (∑REE) abundances are also variable in the soil samples, ranging from 63 to 330 ppm. The PAAS-normalized REE data are arranged in order of increasing atomic number and plotted in a typical diagram (Fig. 2). Additionaly, the samples are grouped according to their REE-normalized patterns. In Group 1 (n = 19), the patterns are characterized by having positive Eu anomalies in most samples (Eu/Eu* = 0.96–1.40), generating convex upward patterns (Fig. 2a). The samples of this group have moderate to high enrichment in light-REE (LREE) and middle-REE (MREE) relative to heavy REE (HREE), numerically expressed as $(La/Yb)_N$ = 1.03–2.90, $(Sm/Yb)_N$ = 1.29–1.95, and $(Sm/La)_N$ = 0.64–1.31. In contrast to Group 1, qualitatively, Group 2 (n = 4) have flat patterns with no-to moderate-enrichment in LREE and MREE relative to HREE ($[La/Yb]_N$ = 0.74–1.42; $[Sm/Yb]_N$ = 0.96–1.17; $[Sm/La]_N$ = 0.82–1.30). The most relevant feature of this pattern is the pronounced negative Eu anomaly (Eu/Eu* = 0.33–0.73; Fig. 2b). Fig. 2a,b shows the distribution patterns of the PAAS-normalized REEs of the sampled rocks.

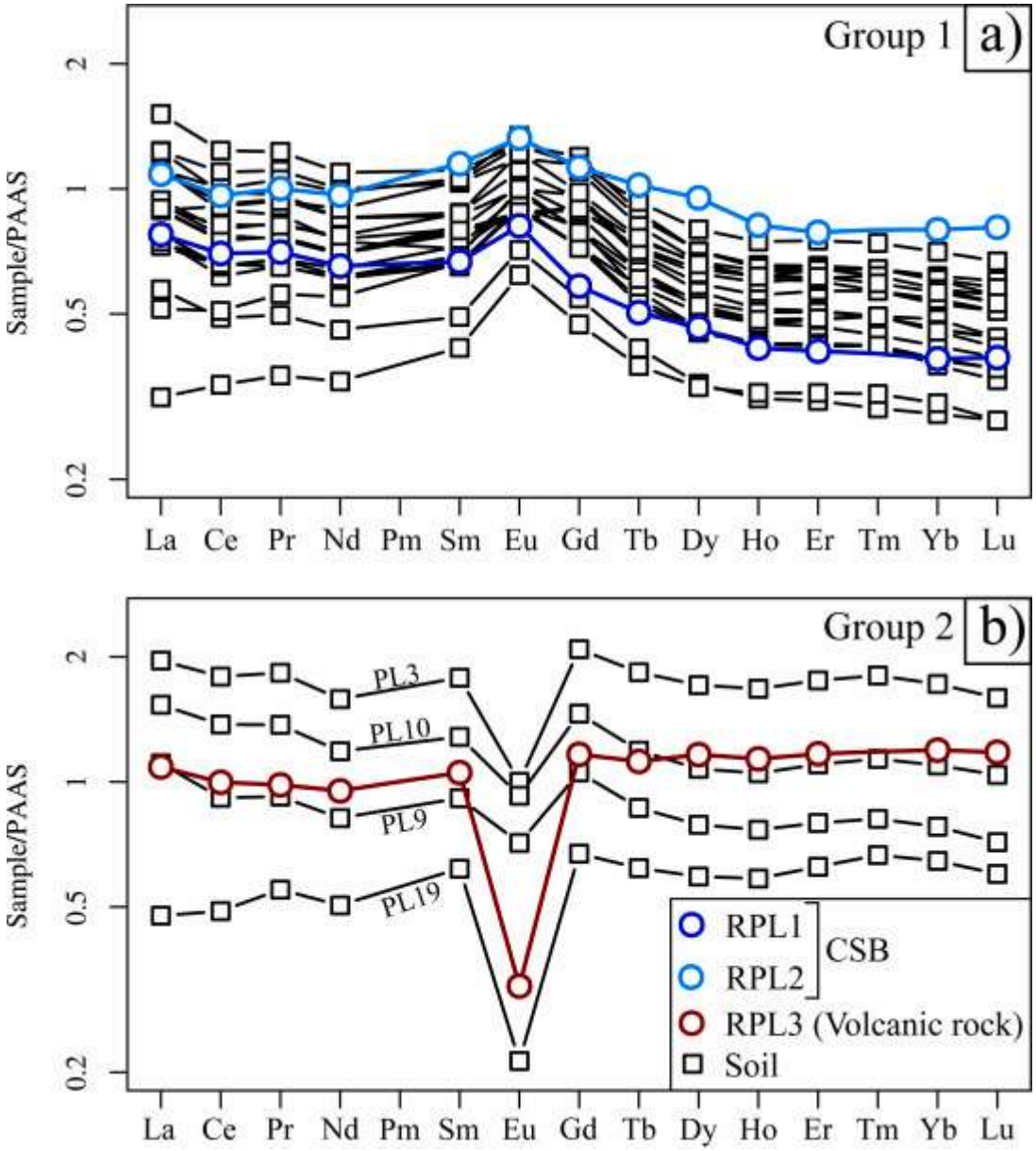

Fig. 2. Distribution patterns of REE concentrations normalized to the PAAS standard values (McLennan, 1989), in the soils of the Puerto Libertad area at the different stations (PL1–PL23). The stations are grouped according to their REE pattern, namely (a) group 1 and (b) group 2 (see text for explanation). CSB: Coastal Sonora Batholith. Rock samples are plotted by comparison.

The mean concentration of PTEs in the soil samples displays the next decreasing order V(141.54 ppm) > Zn(63.65 ppm) > Ni(36.71 ppm) > Cr(29.09 ppm) > Pb(21.46 ppm) > Cu(18.14 ppm) > Co(6.84 ppm) > As(6.34 ppm) > Sn(2.95 ppm) > Mo(2.71 ppm) > Sb(1.08 ppm) > Cd(0.19 ppm). Several PTEs correlate withone another. A significantly positive correlation exists between V and Ni ($\rho = 0.60$; $p = .001$). There is also a significant positive correlation between Ni with Mo ($\rho = 0.52$; $p = .012$), Sn ($\rho = 0.54$; $p = .008$), and Pb ($\rho = 0.50$; $p = .016$). In addition, a significantly positive correlation between Zr and Cr ($\rho = 0.59$; $p = .003$), Pb ($\rho = 0.50$; $p = .017$), Cu ($\rho = 0.47$; $p = .023$), As ($\rho = 0.57$; $p = .004$), Sn ($\rho = 0.42$; $p = .045$), Sb ($\rho = 0.54$; $p = .008$), and Cd ($\rho = 0.78$; $p < .001$) are observed.

3.3. Pollution indices

The average EF values for Zn, Pb, Cu, and Co are less than 2.0. This fact indicates that the soils in the area under research have overall "deficiently to minimal enrichment" in these PTEs. Meanwhile, the resulting average EF values demonstrate that V (EF V = 3.40), Ni (EF Ni = 4.61), Cr (EF Cr = 2.36), Sn (EF Sn = 3.02), Mo (EF Mo = 4.21), and Sb (EF Sb = 2.11) generally have "moderate enrichment" in the soils. The EF data of V, Ni, and Mo in some stations are the highest among the heavy metals (up to 17.54 for V, up to 25.96 for Ni, and up to 14.39 for Mo). They also have "moderate to very high enrichment" in samples located closer to the PLTPP (Fig. 1c), such as PL4, PL8, PL9, PL10, PL14, PL18, PL19, and PL20 (located at less than 3.5 km from the power plant). The farthest samples, namely PL22 (19.1 km) and PL23 (14.7 km), have "minimal enrichment" in most PTEs.

The PI_N is evaluated in this study to assess the mutual contamination effects of the PTEs measured on each soil sample. The comprehensive pollution levels vary among the different samples, ranging from 0.94 to 17.74. The farthest samples from the PLTPP, namely PL22 (PI_N = 1.61) and PL23 (PI_N = 1.58), fall in the "slight pollution" category. Only the sample PL1 (PI_N = 0.94) falls in the "little pollution" category. Meanwhile, the computed average PI_N of the samples under research yields a value of 4.31; it means that, in general, these soils are "serious polluted" by PTEs.

4. Discussion

4.1. Provenance of soils and weathering conditions

One of the issues in environmental research is the establishment of a local geochemical background, which is necessary to quantify the possible anthropogenic impact on soils and sediments (Bern et al., 2019; Calmus et al., 2018; Reimann and de Caritat, 2017; Reimann and Garrett, 2005). The heterogeneities in the soil origin may exert significant impact on individual PTEs and distribution characteristics. The main components of the soils surrounding Puerto Libertad are assumed to be formed from the weathering of the underlying parent rock materials. Because of the semi-arid to arid climate, the soil formation in the region is more influenced by physical rather than chemical weathering. Accordingly, with the dominance of sand-size particles characterizing the samples, the soils are weakly developed, and the organic matter content in the area is very low (avg. = 1.47%). The alkaline pH values are also expected due to the nature of parent rocks and because the vegetation cover is not developed in most parts of the Sonoran Desert (Gutiérrez-Ruacho et al., 2018). Within this environmental context, there is no clear geochemical difference in major and conservative (immobile) elements between rocks, sediments, and soils in the area under research. In this sense, although most diagrams and indices presented here do not discriminate various types of soils, they help discriminate between potential bedrocks and weathering grades.

The major element discriminant function provided by Roser and Korsch (1986) is a method to determine the provenance of soils within single successions, with differentiation into four groups. The Puerto Libertad soils are plotted in the field of felsic igneous provenance with a minor intermediate component (Fig. 3a), typical of rocks derived from silicic crystalline ranges (Roser and Korsch, 1986). In addition, the ratio SiO_2/Al_2O_3 is a commonly employed approach to determine the source and maturity. Higher values of this ratio are related to an increase of quartz at the expense of less resistant components such as feldspar and lithic fragments during transport and recycling. In this regard, the SiO_2/Al_2O_3 ratio is approximately 3.0 in mafic rocks (e.g., basalts and gabbros), and nearly 5.0 in felsic rocks (granites and rhyolites) (Le Maitre et al., 2002; Roser et al., 1996), and more than 6.0 provide evidence of high chemical maturation (Roser et al., 1996). The average value of SiO_2/Al_2O_3 ratio for the studied samples is roughly 5.4, which is suggestive of relatively low maturity and felsic sources. Moreover, the bivariate plot between SiO_2 and $K_2O + Na_2O + Al_2O_3$ (Suttner and Dutta, 1986) reflects a formation under semiarid to arid paleoclimate, thereby indicating weak

chemical weathering (Fig. 3b). The hydraulic sorting of detrital mineral grains can significantly influence the chemical composition of bulk soils. Geochemical variability due to hydraulic sorting can be evaluated using the ICV (Cox et al., 1995; Potter et al., 2005). Rock-forming minerals such as plagioclase, K-feldspars, and amphiboles show ICV values of >0.85, whereas typical alteration products such as kaolinite, illite, and muscovite, exhibit values of <0.85 (Cox et al., 1995; Cullers, 2002). The soil samples from Puerto Libertad have ICV values higher than 0.85, varying from 1.11 to 2.72, indicating that they are enriched in rock-forming minerals. Thus, the plot of CIA vs. ICV (Fig. 3c) displays variance that might be attributed to the same composition of rock source and low degree of alteration. The CIA is used to evaluate the degree of weathering. This index measures the extent to which feldspars have been converted to aluminous weathering products (Fedo et al., 1995; Nesbitt and Young, 1984). The CIA values in the analyzed samples, range from 31.65 to 51.79, and they are plotted in a trend beneath the feldspar join line in the ternary A–CN–K diagram, A: Al_2O_3; CN:CaO × Na_2O; K: K_2O (molar proportions (Fig. 3d). These CIA values indicate that no weathering has occurred and reflect arid climate conditions in the source area (Fedo et al., 1996; Nesbitt et al., 1997).

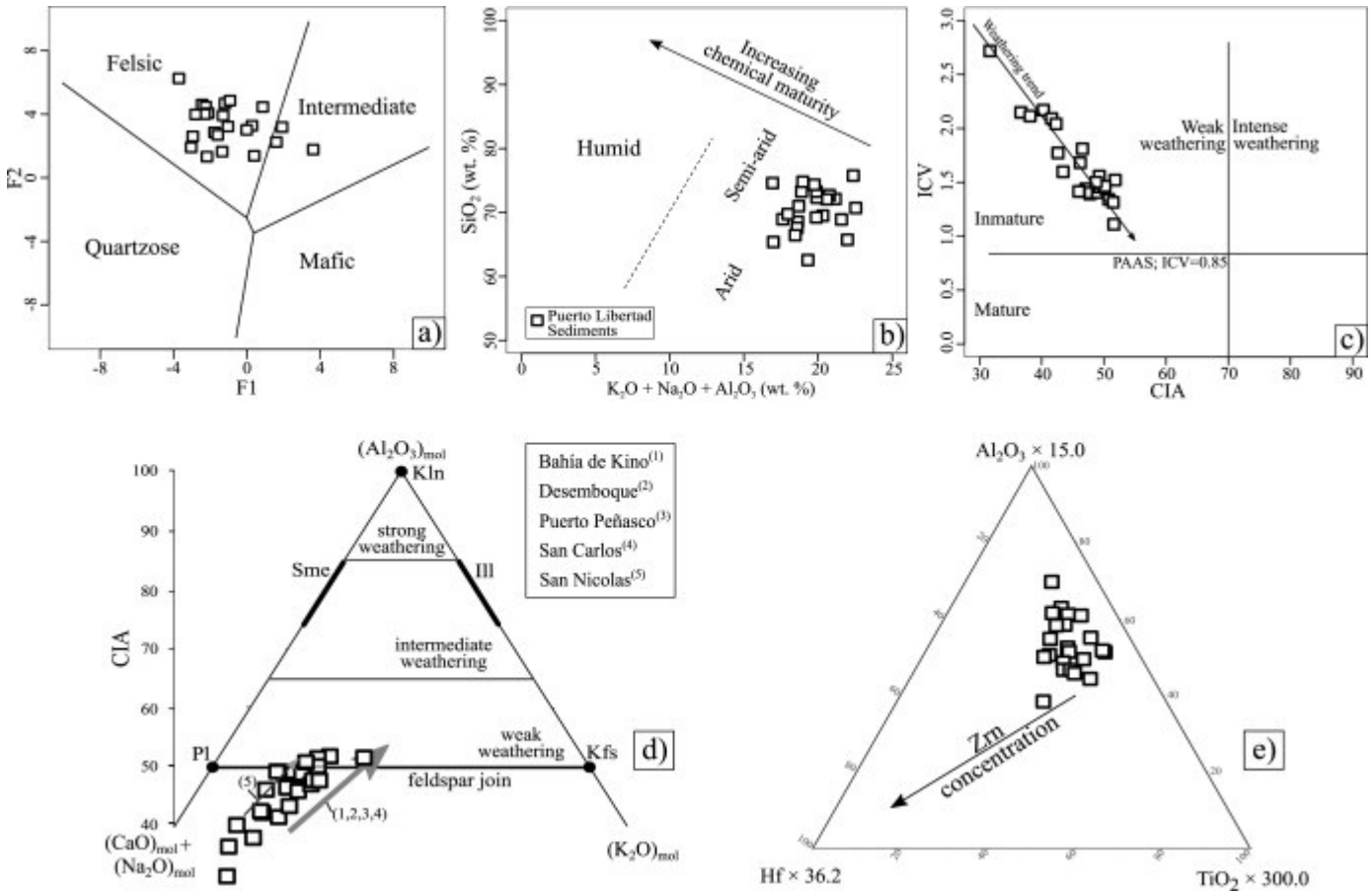

Fig. 3. (a) Classification of the analyzed soils according to the provenance discrimination diagram proposed by Roser and Korsch (1986). The F1 = (−1.773TiO_2 + 0.607Al_2O_3 + 0.76$Fe_2O_3^t$ −1.5MgO + 0.616CaO + 0.509Na_2O −1.224K_2O) − 9.09; F2 = (0.445TiO_2 + 0.07Al_2O_3 − 0.2 $Fe_2O_3^t$ −1.142MgO + 0.438CaO + 1.475Na_2O + 1.426K_2O) − 6.861. (b) Al_2O_3 +K_2O + Na_2O vs. SiO_2 (wt. %) diagram (after Suttner and Dutta, 1986) suggesting a semi-arid climate and an immature chemical nature of the studied sediment samples. (c) The CIA vs. ICV diagram for the sedimentary material from the Puerto Libertad area. (d) The A–CN–K diagram (Nesbitt and Young, 1982) for soil samples from Puerto Libertad. A: Al_2O_3; CN:CaO × Na_2O; K: K_2O (molar proportions). The ternary diagram shows the weathering trend of the beach sands along the Sonoran coast. For comparison, the weathering trend of [1]Bahia de Kino (Armstrong-Altrin, 2009; Madhavaraju et al.,

2016), [2]Desemboque (Madhavaraju et al., 2016), [3]Puerto Peñasco (Madhavaraju et al., 2016), [4]San Carlos (Armstrong-Altrin et al., 2014), and [5]San Nicolas (Armstrong-Altrin et al., 2014) sands are also plotted. (e) The Al_2O_3-Hf-TiO_2 ternary diagram after Murphy (2000) for soil samples around Puerto Libertad (Zrn means zircon).

In assessing the geochemical provenance of the soils, chemically immobile elements are more useful than others are. Some of these elements have an intermediate to relatively high ionic potential and are considered to be chemically immobile under most near-surface environments (e.g., Ti, Al, Zr, Hf, Th and REEs) (Babechuk et al., 2014; Bern et al., 2011; McLennan, 1989; Silva et al., 2018; Taboada et al., 2006). Given that zircon-rich soils preferentially incorporate Hf (and Zr) relative to Al_2O_3 and TiO_2, the accumulation of the zircon-like phases should lead to a specific trend in the ternary Al_2O_3–TiO_2-Hf diagram after Murphy (2000). Such a trend is not shown in the studied samples in the diagram of Fig. 3e. Hence, it is likely that at least the major and immobile element composition of the soils is predominantly controlled by the local weathering of the underlying parent rock, rather than by the secondary sedimentary sorting or reworking of older deposits. According to the abovementioned and range values of the CIA and the ICV in our samples, the lack of evidence of intense paleoweathering at the source suggests that the bulk of the REEs is qualitatively transferred from the source to the unconsolidated material at the surface.

In this sense, REEs are frequently employed as indicators of rock source (Armstrong-Altrin et al., 2014; Madhavaraju et al., 2016; McLennan, 1989; McLennan et al., 1993; Middelburg et al., 1988; Tripathee et al., 2016). On the basis of the REE-normalized diagrams, two geogenic sources are defined. One is the plutonic rock of the CSB belonging to the Laramidic batholitic granitoids (Valencia-Moreno et al., 2011), with clear positive Eu anomaly and similar fractionation of HREE, relative to LREE (Fig. 2a). The other is the rhyolitic Miocene rock dispersedly emplaced around the Sonoran Desert (Olguín-Villa et al., 2013; Stock et al., 1999; Velderrain-Rojas et al., 2021; Vidal-Solano et al., 2007), characterized by the dominant-negative Eu anomalies and flat distributions of the HREE (Fig. 2b). Not surprisingly, the comparison of the REE data of soils with those of likely geogenic components indicates that most samples have received a major contribution from the regional CSB, represented by the samples RPL1 and RPL2. By contrast, the REE patterns of samples like PL3, PL9, PL10, and PL19, are derived mainly from felsic Neogene rocks, geochemically represented by the rock sample RPL3. It is noteworthy that unlike the diverse anomalies in the REEs, weathering, redox, or anthropogenic processes have no remarkable impact on Eu/Eu* values in soils. In this regard, the significant Eu anomalies in our samples can be explained by its geogenic inherited relationship.

4.2. Identification of potentially toxic elements sources

First, to assess the transfer of PTEs from parent rocks to soils, the robust Spearman correlation analysis between Zr and PTEs is utilized to test this inference. Zirconium is generally considered to be geochemically immobile in soils because it has low water solubility and has a great affinity to refractory minerals such as zircon ($ZrSiO_4$) and baddeleyite (ZrO_2) (Middelburg et al., 1988; Taboada et al., 2006). Therefore, the elements linked with Zr must have been derived from geogenic sources such as rock weathering and erosion at the sampling sites. The statistical results present significant correlation coefficient values ($p < .05$) between Zr and several PTEs, such as Cr, Pb, Cu, As, Sn, Sb, and Cd, revealing a commonality among these elements (Table 6S). This result is congruent with the fact that these elements in the soils fall mainly in the EF class, delimiting "deficiently to minimal enrichment" ($EF < 2$). These features indicate that the concentration of these PTEs is mainly inherited from the bedrock and that a natural enrichment could occur in sites with EF values greater than 1.

The identification of anthropogenic pollution sources is an issue (Cabral Pinto et al., 2017; Paladino et al., 2017; Reimann and Garrett, 2005). By the computation of pollution indices in soils, some insight can be provided on the sources and sites of PTEs accumulation. In our case, the first thing to highlight is the elevated PTEs concentrations found at the stations close to Puerto Libertad, especially those in the immediate vicinity of the PLTPP, such as PL4, PL8, PL9, PL10, and PL20 (ΣPTEs between 312.56 and 769.84 ppm). On the contrary, the concentrations of PTEs, and EF values, are generally lower in the more remote sites from the power plant. The sampling points PL6, PL22, and PL23 are the clear examples of this observation (Fig. 1c). Through this, a simple geographic observation is recognized as a pattern capable of constraining the source of the anthropogenic PTEs enrichment in the soils directly related to the PLPP activities (point-source pollution).

The combustion of heavy oils produces byproducts that are characterized by a high content of PTEs, mainly V and Ni, and other non-burnt components (e.g., Bosco et al., 2005; Moreno et al., 2010, 2008). Gupta and Krishnamurthy (1992) reported the chemical composition of ROFA from various origins and observed a great diversity in V and Ni compositions 2.5%–40% for V_2O_5 and 0.8%–6% for NiO. On the basis of a review of 10 studies on the chemistry of metal concentration in emissions generated by oil fuel power plants worldwide, Pastrana-Corral et al. (2017) found that V varies in such emissions between 0.3% and 6.1% and that Ni ranges between 0.0016% and 1.4%. For its part, Navarro et al. (2007) analyzed the metal contents of oil fly ash from a thermal power plant installed in Mexico. They also found contents measured as weight percentages for V (1.6%) and Ni (0.85%). This indicates that the fly ash emitted by the power plants is a common source of these metals and that soils in the surrounding areas can be the repositories of these PTEs generated through oil burned. In this investigation, the main hypothesis is that the concentrations of those elements in the studied soils are influenced by residual matter from fossil fuel combustion as a primary industrial-type activity in the surveyed area. Significant traffic contributions, as well as agricultural and metal and metalloid mining, can be ruled out. Average EF values for V and Ni are the highest among the PTEs (avg. EFV = 2.55; avg. EFNi = 3.33). Moreover, given that V and Ni present a high positive correlation ($\rho = 0.60$; $p = .001$), it is likely that their enrichment has a common source. As the processes of the power station represent the main anthropogenic activity, the chemical compositions of the soils could be influenced by the byproducts of the PLTPP. In addition, despite the very low contents of OM in the soils under study, the strong positive correlation between the OM and V ($\rho = 0.63$; $p = .002$) and Ni ($\rho = 0.58$; $p = .004$) indicates an association of organic ligands with the retention and low mobility of these metals even in an arid environment.

The primary anthropogenic source of V and Ni in the samples is also recognized with the aid of ternary diagrams. The La(× 3.1)-Ce(× 1.54)-V ternary graph is used to compare geochemical signatures from crustal, refinery, and oil-fired power station and industrial district emissions (Moreno et al., 2008). The soil samples define a linear trend ranging from the local crustal component, namely the rock sample analyzed in the area, to increasing V-rich compositions (ROFA-like end member, Fig. 4a). In addition, the V–Ni–La(× 10) ternary diagram is employed to contrast the crustal sources of atmospheric particulate matter from fuel oil/ROFA contribution, which lie toward the La-vertex, with ratios more strongly influenced by hydrocarbon combustion (Moreno et al., 2010). In the V–Ni–La(× 10) triangle (Fig. 4b), the studied samples plotted in a trend from the crustal components to the V–Ni range line (V/Ni = 1–3) represent the fuel oil and their residual fly ash combustion. The interpretation of the linear trend of the samples on Fig. 4a and 4b, due to the primarily anthropogenic influence of Ni- and/or V-bearing particulate, suggests that those elements are derived from hydrocarbon combustion within the power plant.

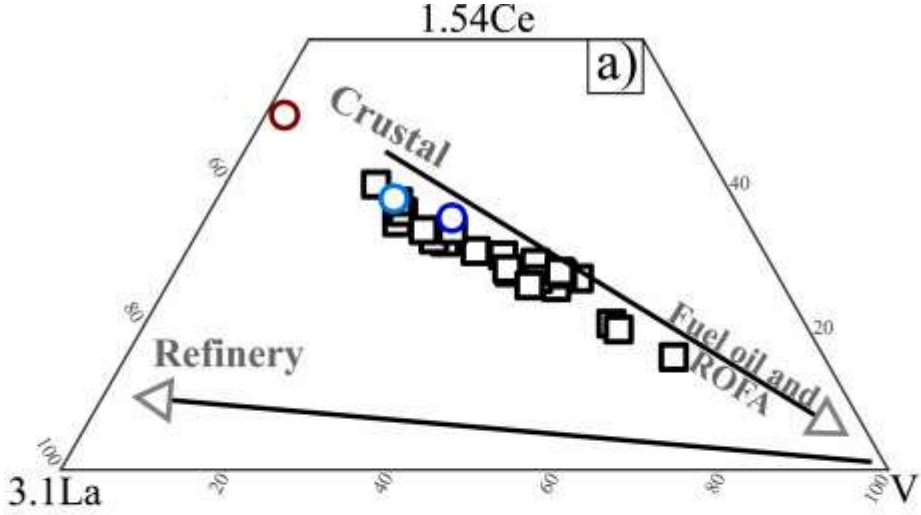
1.54Ce
a)
Crustal
Fuel oil and ROFA
Refinery
3.1La
V

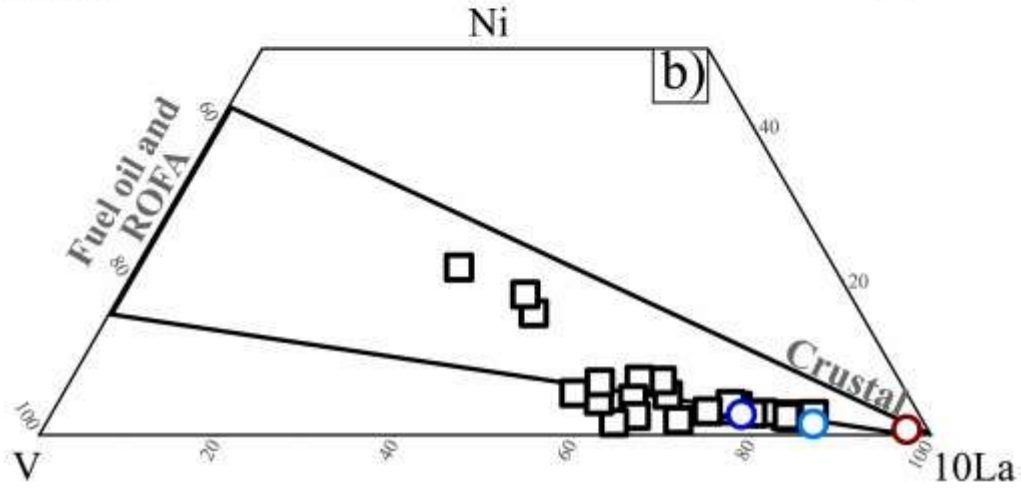
Ni
b)
Fuel oil and ROFA
Crustal
V
10La

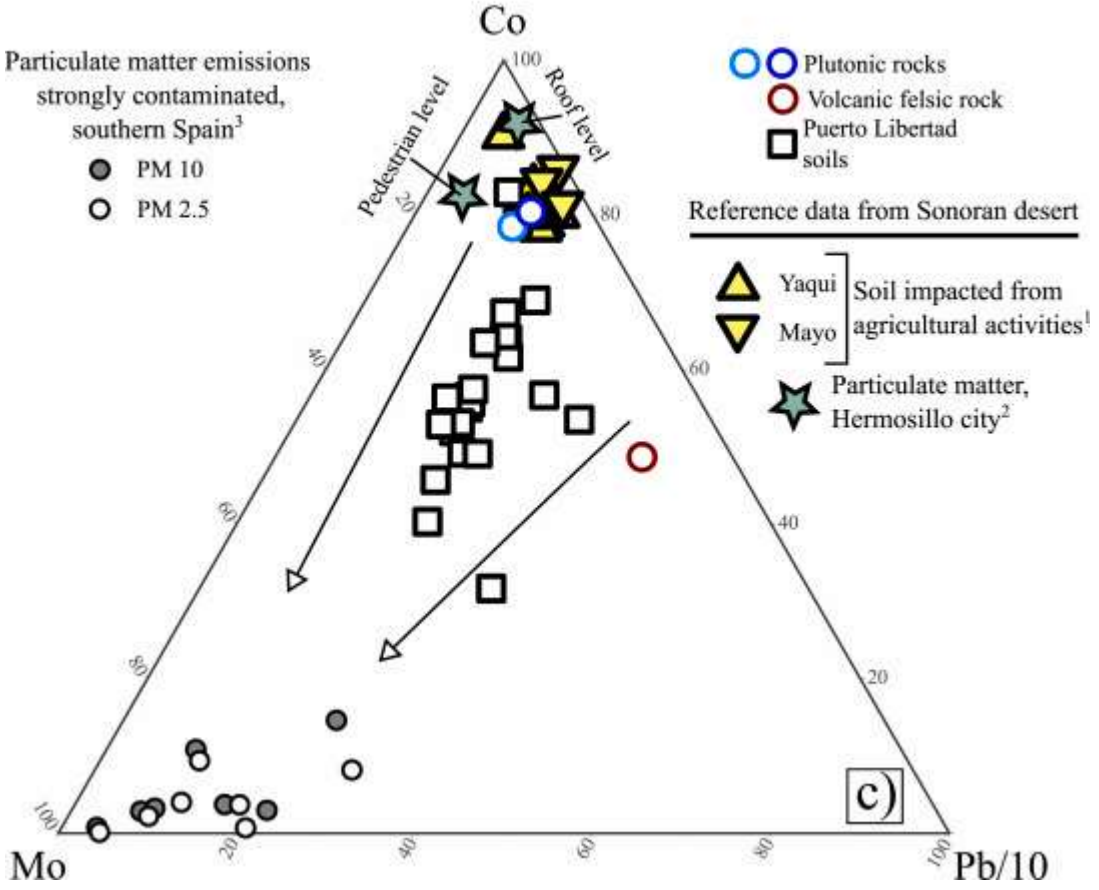
Co
Particulate matter emissions strongly contaminated, southern Spain[3]
PM 10
PM 2.5
Pedestrian level
Roof level
Plutonic rocks
Volcanic felsic rock
Puerto Libertad soils
Reference data from Sonoran desert
Yaqui
Mayo
Soil impacted from agricultural activities[1]
Particulate matter, Hermosillo city[2]
c)
Mo
Pb/10

Fig. 4. (a) La(× 3.1) –Ce(× 1.54) –V (Moreno et al., 2008) and (b) V–Ni–La(× 10) (Moreno et al., 2010) diagrams applied to the soils under study. The smaller triangle in (b) represents the compositional range of the V/Ni ratio of fuel oil and residual fly ash combustion after (Moreno et al., 2010). The rock values analyzed in this study are included for references. (c) The ternary diagram for (Mo–Co–Pb × 0.1). Reference values are reported to [1]the average local crustal component (plutonic and volcanic rocks), [1]soil impacted from agricultural activities in Sonora (Meza-Montenegro et al., 2012), [2]atmospheric particulate matter from the urban area of Hermosillo, Sonora (Meza-Figueroa et al., 2016), and [3]atmospheric particulate matter strongly contaminated from industrial districts (Moreno et al., 2008, 2010).

Based on the significant correlation found between Ni and Mo ($\rho = 0.52$; $p = .05$), as well as the high average EFMo (3.38) in the Puerto Libertad soils, the idea that the fly ash emitted by the PLTPP is a potential source of the enrichment of this element in soils has emerged. The Mo–Co–Pb/10 ternary diagram can discriminate between different natural and anthropogenic sources (Zheng et al., 2016). The reference values of soil and atmospheric particulate matter from impacted agricultural and urban activities in Sonora are illustrated in this triangle (Fig. 4c) (Meza-Figueroa et al., 2016; Meza-Montenegro et al., 2012). On the plot, the soil samples of this investigation define a trend between two end members again, namely geogenic and anthropogenic compositions. The crustal component is near the Co-rich apex. The anthropogenic end-member, marked by atmospheric particulate matter strongly contaminated by refinery emissions (PM2.5 and PM10; Moreno et al., 2010, 2008), is plotted on the Co- and Pb-depleted but Mo-enriched end. The samples of Puerto Libertad present a linear trend with a tendency to the particulate matter emission behavior, which also confirms that, the main anthropogenic contribution in the research area comes from the combustion of fossil fuels. Our findings would seem to show that moderate Mo enrichment could be considered a marker of residual heavy oil emissions.

The interpretation of the sources of the metals and metalloids from PCA analysis resembles the correlation analysis results (Table 7S) and the ternary diagrams above presented, thereby corroborating the interpretation about the origin of the PTEs in this research. In agreement with the three component matrices (cumulative variance of ~64.4%) plotted in a 3-D diagram (Fig. 4S), four distinct clusters can be identified. (i) The cluster forming by V and Ni has created an impression that has a major anthropogenic influence that controls the distribution of these metals. (ii) The correlated elements in the PCA, namely, Sb, Cu, Cd, As, and Cr, suggest a common source. (iii) Furthermore, Pb, Sn, and Co form another set of elements. The strong correlation between Zr and elements of these groups may reflect mostly their geogenic source. However, they are separated by a long distance in the 3-D PCA loading plot, which suggests different lithological or natural sources. (iv) The group of elements formed by Zn and Mo is considered intermediate, which is interpreted to have sources controlled mainly by anthropogenic inputs but with some geogenic influence.

4.3. Potential influence of the Puerto Libertad power plant on the Sonoran Desert

The ROFA can settle out rapidly, attaining the highest pollution markers in soils at 5–8 km from an oil-fired thermoelectric plant (Ganor et al., 1988; Mazhaiskii et al., 2000; Pastrana-Corral et al., 2017). The integrated pollution indices allow the assessment of the overall level of soil pollution (Table 8S), considering the content of all the PTEs. The PIN has turned out to be essential for this purpose. In this regard, a bubble map is displayed based on the regulated trigger points of this index (Fig. 5). The distribution of the PIN for the surveyed soils reflects high anthropogenic loads (PIN >3) in the immediate vicinity of Puerto Libertad. This feature also determines a strong proof to associate source point pollution emissions from the power plant and confirms the stronger environmental affectation in their immediacy. An exception is the sample PL3, as it has a PIN value of 5.84 and occurs 9.7 km to the north of the PLTPP, but the main body of emissions goes to the east and southeast

of the power plant in accordance with the wind direction patterns (Fig. 1b). This anomaly can be explained because this sample is more sensitive to an environment perturbation due to the nature of their parent rock (volcanic felsic rock).

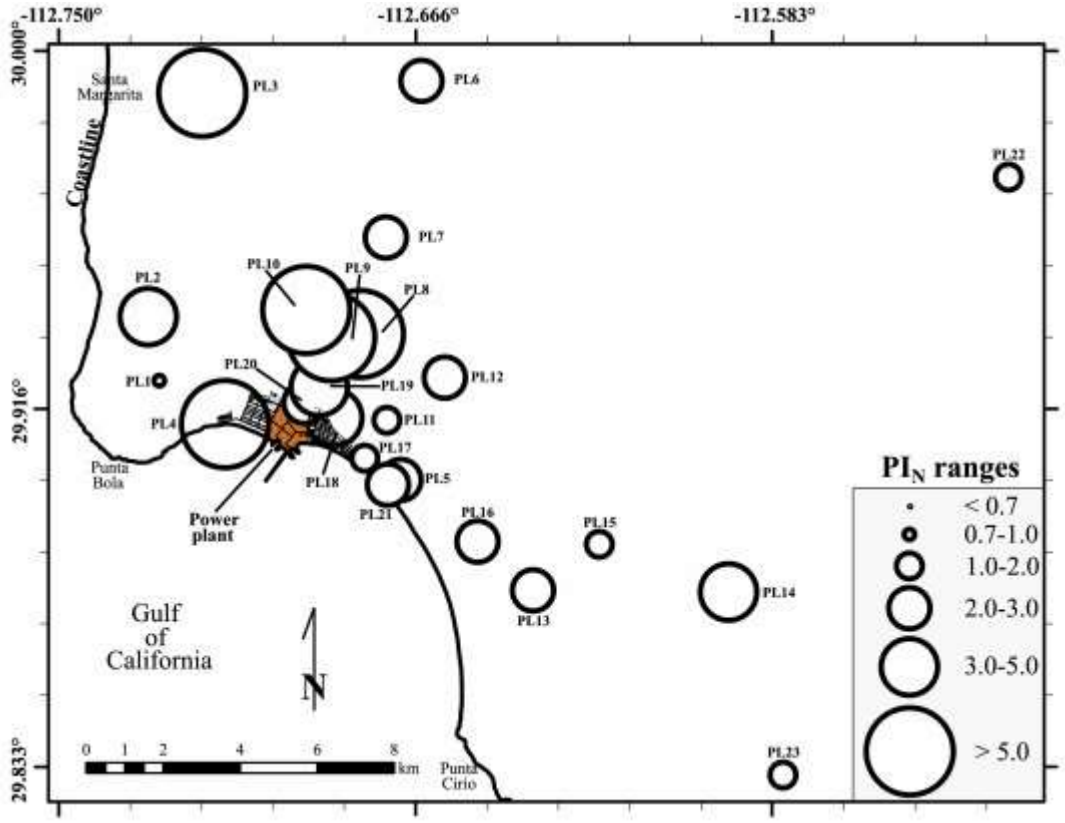

Fig. 5. Bubble map showing the spatial distribution of the Nemerow integrated pollution index in soils around Puerto Libertad.

The extent of pollution is not limited to the vicinity of the source, as aerosols are transported into the atmosphere, and even previously deposited contaminated materials may be physically remobilized by winds, particularly during times of drought, thereby causing the dispersion of the pollutant over many kilometers from the source (Liu et al., 2018; Wang et al., 2008). The most significant factors for distributing pollutants are meteorological parameters such as precipitation and wind speed and direction (Liu et al., 2018; Meza-Figueroa et al., 2007; Moreno-Rodríguez et al., 2015; Yang et al., 2017). The potential influence area of the power plant on the Sonoran Desert is displayed in the air forward trajectory models (HYSPLIT) from Puerto Libertad (Fig. 6). The long-range influence zone covers a wide area east of the Gulf of California. Given the large variability of factors such as spatio-temporal distribution and the magnitude of the pollutant mass involved, it is likely that the fall out of the pollutant material is not uniformly distributed into the terrain. How the main body of the emissions of the plant affects air quality and soils in the long-range vulnerable region remains unknown. The large volumes of precipitation of the North American Monsoon may dilute and mitigate the atmospheric particulate that carries PTEs (Liu et al., 2020; Moreno-Rodríguez et al., 2015; Thorpe and Harrison, 2008). Conversely, the PTEs can be gathered along a specific direction by the wind. In such a complicated scenario, it is further vital to reveal the relationship between source-area pollution, meteorological conditions, timing, and the transport of pollutants into the Sonoran Desert.

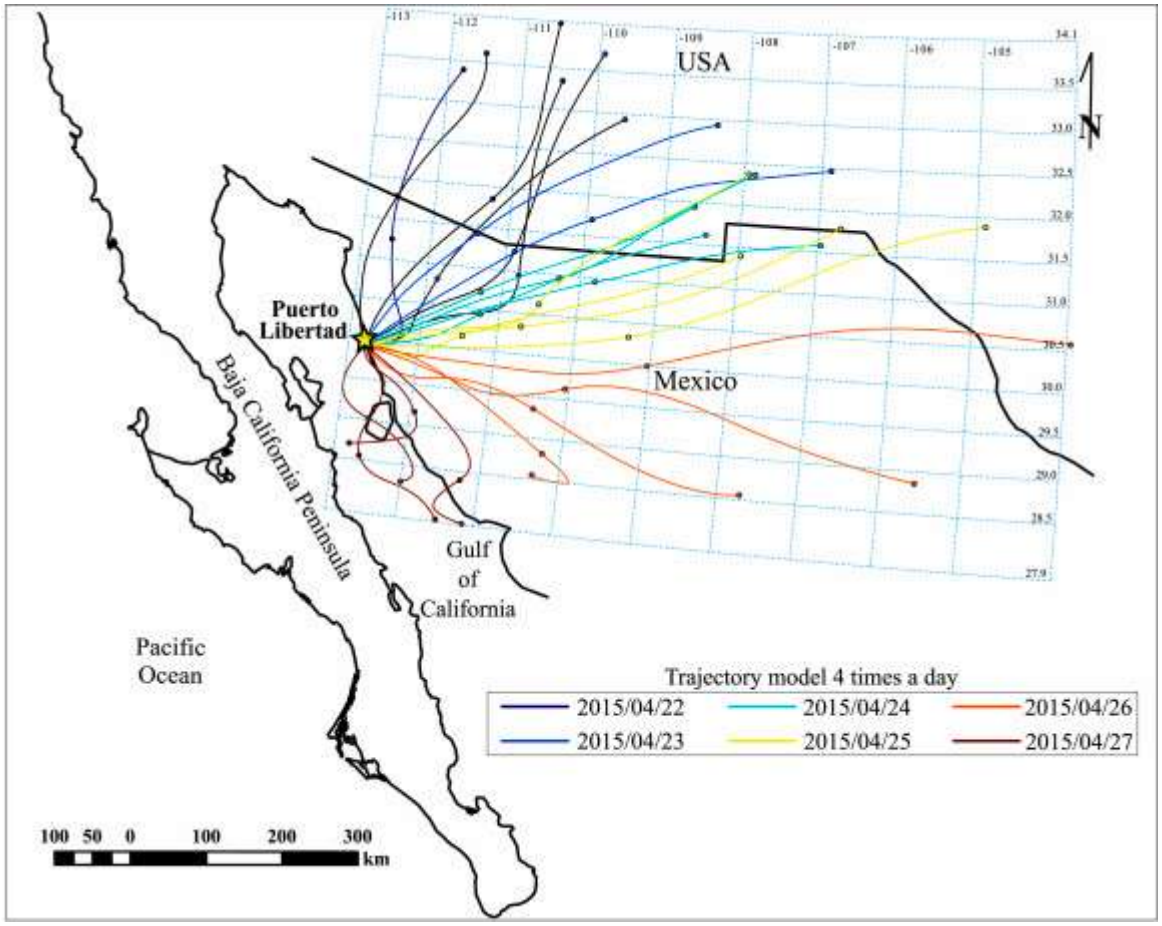

Fig. 6. Air mass forward trajectory models four times a day for six days in 2015 using the CRAN OpenAir (v.2.8.1) (Carslaw and Ropkins, 2012). The starting point coordinates are latitude = 29.9058, longitude = −112.6928, with a height of 100 m.a.s.l. For the interpretation of the references to colors in the legend, the reader is referred to the web version of this paper. (For interpretation of the references to color in this figure legend, the reader is referred to the Web version of this article.)

5. Conclusions

It has been demonstrated that the topsoil around Puerto Libertad is influenced by natural and anthropogenic sources. Major oxides and immobile trace elements (presented as elemental ratios, discriminant-function, bivariate, and ternary plots) reveal that (i) the soils are derived from intermediate to felsic source rocks; (ii) their geochemical compositions are predominantly controlled by the local weathering of the bedrock as immature soils; and (iii) they are formed under a low degree of chemical weathering under semiarid/arid conditions. The lanthanides are qualitatively well preserved in the soils and are a reliable indicator of their parent rock. The PAAS-normalized REE patterns indicate two likely geogenic sources that outcrop in the research area: (i) Laramidic plutonic rocks and (ii) Neogene volcanic felsic rocks. The EF and statistical analyses (nonparametric correlations and PCA) are combined with spatial distribution patterns to identify the sources of PTEs and classify them on the basis of their sources as geogenic or anthropogenic. The results confirm that a considerable portion of V and Ni in the soils has an anthropogenic origin. In the cases of Zn and Mo, they are significantly influenced by anthropogenic inputs. By contrast, the chemical concentrations of the remaining PTEs (Sb, Pb, Sn, Cu, Cd, As, Cr, and Co) are mainly associated with the parent bedrock. According to ternary diagrams, it is confirmed that the enrichment of V, Ni, and Mo has its source from the fly ash generated in the power plant housed in the research area during

the period when this plant has been operated with fuel oil. In addition, the interpretation based on air forward trajectory models indicates a wide area of the potential influence of the atmospheric particulate generated in the power plant into the Sonoran Desert.

Declaration of competing interest

The authors declare that they have no known competing financial interests or personal relationships that could have appeared to influence the work reported in this paper.

Acknowledgments

This work was performed within the framework of the development of the SLE-CT(CICESE) in collaboration with INGV. This research was made possible by a postdoctoral grant from SENER-CONACyT. We thank to Ramon Alfonso Pérez-Ruiz and his son for their help in the field. Many thanks also to Vladimir Mendoza-Lavaniegos (CICESE) for technical assistance in the acquisition of major elements data. Special acknowledgements to Vojtěch Ettler and Gildas Ratié for revising a preliminary version of this manuscript and giving great and constructive comments and suggestions. Careful and constructive comments from the guest editor and three anonymous referees are also greatly appreciated.

Appendix A. Supplementary data

The following is the Supplementary data to this article:

Download : Download Word document (3MB)

References

Adams and Comrie, 1997
D.K. Adams, A.C. Comrie
the North American Monsoon
Bull. Am. Meteorol. Soc., 78 (1997), pp. 2197-2214, 10.1175/1520-0477(1997)078<2197:TNAM>2.0.CO;2
View Record in ScopusGoogle Scholar

Aguilar-Hinojosa et al., 2016
Y. Aguilar-Hinojosa, D. Meza-Figueroa, A.I. Villalba-Atondo, M.A. Encinas-Romero, J.L. Valenzuela-García, A. Gómez-Álvarez
Mobility and bioavailability of metals in stream sediments impacted by mining activities: the jaralito and the Mexicana in Sonora, Mexico. Water. Air
Soil Pollut., 227 (2016), p. 345, 10.1007/s11270-016-3046-1
View Record in ScopusGoogle Scholar

Al-Degs et al., 2014
Y.S. Al-Degs, A. Ghrir, H. Khoury, G.M. Walker, M. Sunjuk, M.A. Al-Ghouti
Characterization and utilization of fly ash of heavy fuel oil generated in power stations
Fuel Process. Technol., 123 (2014), pp. 41-46, 10.1016/j.fuproc.2014.01.040
Article
Download PDFView Record in ScopusGoogle Scholar

Al-Ghouti et al., 2011
M.A. Al-Ghouti, Y.S. Al-Degs, A. Ghrair, H. Khoury, M. Ziedan

Extraction and separation of vanadium and nickel from fly ash produced in heavy fuel power plants
Chem. Eng. J., 173 (2011), pp. 191-197, 10.1016/j.cej.2011.07.080
Article
Download PDFView Record in ScopusGoogle Scholar

Allouis et al., 2003
C. Allouis, F. Beretta, A. D'Alessio
Structure of inorganic and carbonaceous particles emitted from heavy oil combustion
Chemosphere, PIC7 51 (2003), pp. 1091-1096, 10.1016/S0045-6535(02)00714-2
Article
Download PDFView Record in ScopusGoogle Scholar

Alloway, 2013
B.J. Alloway
Sources of heavy metals and metalloids in soils
B.J. Alloway (Ed.), Heavy Metals in Soils: Trace Metals and Metalloids in Soils and Their Bioavailability, Environmental Pollution, Springer Netherlands, Dordrecht (2013), pp. 11-50, 10.1007/978-94-007-4470-7_2
View Record in ScopusGoogle Scholar

Al-Masri et al., 2015
M.S. Al-Masri, Haddad, Kh, N. Alsomel, A. Sarhil
Neutron activation analysis of thermal power plant ash and surrounding area soils
Environ. Monit. Assess., 187 (2015), p. 536, 10.1007/s10661-015-4771-4
View Record in ScopusGoogle Scholar

Amundson, 2014
R. Amundson
soil formation
H.D. Holland, K.K. Turekian (Eds.), Treatise on Geochemistry (second ed.), Elsevier, Oxford (2014), pp. 1-26, 10.1016/B978-0-08-095975-7.00501-5
Article
Download PDFView Record in ScopusGoogle Scholar

Armstrong-Altrin, 2009
J.S. Armstrong-Altrin
Provenance of sands from cazones, acapulco, and bahía Kino beaches, Mexico
Rev. Mex. Ciencias Geol., 26 (2009), pp. 764-782
View Record in ScopusGoogle Scholar

Armstrong-Altrin et al., 2014
J.S. Armstrong-Altrin, R. Nagarajan, Y.İ. Lee
Geochemistry of sands along the San Nicolás and San Carlos beaches, Gulf of California, Mexico: implications for provenance and tectonic setting
Turk. J. Earth Sci., 23 (2014), pp. 533-558, 10.3906/yer-1309-21
View Record in ScopusGoogle Scholar

Babechuk et al., 2014
M. Babechuk, M. Widdowson, B. Kamber
Quantifying chemical weathering intensity and trace element release from two contrasting basalt profiles, Deccan Traps, India
Chem. Geol., 363 (2014), pp. 56-75, 10.1016/j.chemgeo.2013.10.027
Article
Download PDFView Record in ScopusGoogle Scholar

Bern et al., 2011
C.R. Bern, O.A. Chadwick, A.S. Hartshorn, L.M. Khomo, J. Chorover

A mass-balance model to separate and quantify colloidal and solute redistributions in soil
Chem. Geol., 282 (2011), pp. 113-119, 10.1016/j.chemgeo.2011.01.014
Article
Download PDFView Record in ScopusGoogle Scholar

Bern et al., 2019
C.R. Bern, K. Walton-Day, D.L. Naftz
Improved enrichment factor calculations through principal component analysis: examples from soils near breccia pipe uranium mines, Arizona, USA
Environ. Pollut., 248 (2019), pp. 90-100, 10.1016/j.envpol.2019.01.122
Article
Download PDFView Record in ScopusGoogle Scholar

Boix et al., 2001
A. Boix, J. Manuel Miguel, X. Querol, T. Sanfeliu
Characterization of total suspended particles around a power station in an urban coastal area in eastern Spain
Environ. Geol., 40 (2001), pp. 891-896, 10.1007/s002540100249
View Record in ScopusGoogle Scholar

Bosco et al., 2005
M.L. Bosco, D. Varrica, G. Dongarrà
Case study: inorganic pollutants associated with particulate matter from an area near a petrochemical plant
Environ. Res., 99 (2005), pp. 18-30, 10.1016/j.envres.2004.09.011
Article
Download PDFView Record in ScopusGoogle Scholar

Buat-Menard and Chesselet, 1979
P. Buat-Menard, R. Chesselet
Variable influence of the atmospheric flux on the trace metal chemistry of oceanic suspended matter
Earth Planet Sci. Lett., 42 (1979), pp. 399-411, 10.1016/0012-821X(79)90049-9
Article
Download PDFView Record in ScopusGoogle Scholar

Cabral Pinto et al., 2017
M. Cabral Pinto, M. Silva, E. Silva, P. Dinis, F. Rocha
Transfer processes of potentially toxic elements (PTE) from rocks to soils and the origin of PTE in soils: a case study on the island of Santiago (Cape Verde)
J. Geochem. Explor., 183 (2017), 10.1016/j.gexplo.2017.06.004
Google Scholar

Cai et al., 2015
L. Cai, Z. Xu, P. Bao, M. He, L. Dou, L. Chen, Y. Zhou, Y.-G. Zhu
Multivariate and geostatistical analyses of the spatial distribution and source of arsenic and heavy metals in the agricultural soils in Shunde, Southeast China
J. Geochem. Explor., 148 (2015), pp. 189-195, 10.1016/j.gexplo.2014.09.010
Article
Download PDFView Record in ScopusGoogle Scholar

Calmus et al., 2018
T. Calmus, M.V. Moreno, R.D.R. Salas, L. Ochoa-Landín, H.M. Quijada
A multi-elemental study to establish the natural background and geochemical anomalies in rocks from the Sonora river upper basin, NW Mexico
Rev. Mex. Ciencias Geol., 35 (2018), pp. 158-178
CrossRefView Record in ScopusGoogle Scholar

Carslaw and Ropkins, 2012
D. Carslaw, K. Ropkins
Openair --- an R package for air quality data analysis
Environ. Model. Software, 27--28 (2012), pp. 52-61, 10.1016/j.envsoft.2011.09.008
Article
Download PDFView Record in ScopusGoogle Scholar
Christensen et al., 2018
E.R. Christensen, E. Steinnes, O.A. Eggen
Anthropogenic and geogenic mass input of trace elements to moss and natural surface soil in Norway
Sci. Total Environ., 613–614 (2018), pp. 371-378, 10.1016/j.scitotenv.2017.09.094
Article
Download PDFView Record in ScopusGoogle Scholar
Cox et al., 1995
R. Cox, D.R. Lowe, R.L. Cullers
The influence of sediment recycling and basement composition on evolution of mudrock chemistry in the southwestern United States
Geochem. Cosmochim. Acta, 59 (1995), pp. 2919-2940, 10.1016/0016-7037(95)00185-9
Article
Download PDFView Record in ScopusGoogle Scholar
Cullers, 2002
R.L. Cullers
Implications of elemental concentrations for provenance, redox conditions, and metamorphic studies of shales and limestones near Pueblo, CO, USA
Chem. Geol., 191 (2002), pp. 305-327, 10.1016/S0009-2541(02)00133-X
Article
Download PDFView Record in ScopusGoogle Scholar
Dinis et al., 2021
L. Dinis, C. Bégin, M.M. Savard, M. Parent
Impacts of smelter atmospheric emissions on forest nutrient cycles: evidence from soils and tree rings
Sci. Total Environ., 751 (2021), p. 141427, 10.1016/j.scitotenv.2020.141427
Article
Download PDFView Record in ScopusGoogle Scholar
Dorn, 2011
R.I. Dorn
Revisiting dirt cracking as a physical weathering process in warm deserts
Geomorphology, 135 (2011), pp. 129-142, 10.1016/j.geomorph.2011.08.010
Article
Download PDFView Record in ScopusGoogle Scholar
Duffus, 2002
J.H. Duffus
“Heavy metals” a meaningless term? (IUPAC Technical Report)
Pure Appl. Chem., 74 (2002), pp. 793-807, 10.1351/pac200274050793
Google Scholar
Fedo et al., 1996
C. Fedo, K. Eriksson, E. Krogstad
Geochemistry of shales from the archean (~3.0 Ga) buhwa greenstone belt, Zimbabwe: implications for provenance and source-area weathering
https://doi.org/10.1016/0016-7037(96)00058-0 (1996)
Google Scholar

Fedo et al., 1995
C.M. Fedo, H.W. Nesbitt, G.M. Young
Unraveling the effects of potassium metasomatism in sedimentary rocks and paleosols, with implications for paleoweathering conditions and provenance
Geology, 23 (1995), pp. 921-924, 10.1130/0091-7613(1995)023<0921:UTEOPM>2.3.CO;2
View Record in ScopusGoogle Scholar
Franco-Uría et al., 2009
A. Franco-Uría, C. López-Mateo, E. Roca, M.L. Fernández-Marcos
Source identification of heavy metals in pastureland by multivariate analysis in NW Spain
J. Hazard Mater., 165 (2009), pp. 1008-1015, 10.1016/j.jhazmat.2008.10.118
Article
Download PDFView Record in ScopusGoogle Scholar
Galán et al., 2014
E. Galán, I. González, A. Romero, P. Aparicio
A methodological approach to estimate the geogenic contribution in soils potentially polluted by trace elements. Application to a case study
J. Soils Sediments, 14 (2014), pp. 810-818, 10.1007/s11368-013-0784-1
View Record in ScopusGoogle Scholar
Ganor et al., 1988
E. Ganor, S. Altshuller, H.A. Foner, S. Brenner, J. Gabbay
Vanadium and nickel in dustfall as indicators of power plant pollution
Water, Air, Soil Pollut., 42 (1988), pp. 241-252, 10.1007/BF00279270
View Record in ScopusGoogle Scholar
García-Rico et al., 2016
L. García-Rico, D. Meza-Figueroa, A. Jay Gandolfi, R. Del Río-Salas, F.M. Romero, M.M. Meza-Montenegro
Dust–metal sources in an urbanized arid zone: implications for health-risk assessments
Arch. Environ. Contam. Toxicol., 70 (2016), pp. 522-533, 10.1007/s00244-015-0229-5
View Record in ScopusGoogle Scholar
Gastil and Krummenacher, 1977
R.G. Gastil, D. Krummenacher
Reconnaissance geology of coastal Sonora between Puerto lobos and bahia Kino
GSA Bull., 88 (1977), pp. 189-198, 10.1130/0016-7606(1977)88
<189:RGOCSB>2.0.CO;2
View Record in ScopusGoogle Scholar
Gaudette et al., 1974
H.E. Gaudette, W.R. Flight, L. Toner, D. Folger
An inexpensive titration method for the determination of organic carbon in recent sediments
https://doi.org/10.1306/74D729D7-2B21-11D7-8648000102C1865D (1974)
Google Scholar
globalenergyobservatory, 2002
globalenergyobservatory
[WWW Document], 3.8.21
http://globalenergyobservatory.org/form.php?pid=4958 (2002)
URL
González-Grijalva et al., 2019
B. González-Grijalva, D. Meza-Figueroa, F.M. Romero, A. Robles-Morúa, M. Meza-Montenegro, L. García-Rico, R. Ochoa-Contreras

The role of soil mineralogy on oral bioaccessibility of lead: implications for land use and risk assessment
Sci. Total Environ., 657 (2019), pp. 1468-1479, 10.1016/j.scitotenv.2018.12.148
Article
Download PDFView Record in ScopusGoogle Scholar

Gray et al., 2003
C.W. Gray, R.G. McLaren, A.H.C. Roberts
Atmospheric accessions of heavy metals to some New Zealand pastoral soils
Sci. Total Environ., 305 (2003), pp. 105-115, 10.1016/S0048-9697(02)00404-7
Article
Download PDFView Record in ScopusGoogle Scholar

Gupta and Krishnamurthy, 1992
C.K. Gupta, N. Krishnamurthy
Extractive Metallurgy of Vanadium
Elsevier (1992)
Google Scholar

Gutiérrez-Ruacho et al., 2018
O. Gutiérrez-Ruacho, M.L. Coronado, F. Sánchez-Teyer, A. Sánchez, A. Gutiérrez, M. Esqueda, O. Gutiérrez-Ruacho, M.L. Coronado, F. Sánchez-Teyer, A. Sánchez, A. Gutiérrez, M. Esqueda
Abundance of rhizospheric bacteria and fungi associated with Fouquieria columnaris at Punta Cirio, Sonora, Mexico
Rev. Mex. Biodivers., 89 (2018), pp. 541-552, 10.22201/ib.20078706e.2018.2.1620
View Record in ScopusGoogle Scholar

Häsänen et al., 1986
E. Häsänen, V. Pohjola, M. Hahkala, R. Zilliacus, K. Wickström
Emissions from power plants fueled by peat, coal, natural gas and oil
Sci. Total Environ., 54 (1986), pp. 29-51, 10.1016/0048-9697(86)90254-8
Article
Download PDFView Record in ScopusGoogle Scholar

Heidari et al., 2021
M. Heidari, T. Darijani, V. Alipour
Heavy metal pollution of road dust in a city and its highly polluted suburb; quantitative source apportionment and source-specific ecological and health risk assessment
Chemosphere, 273 (2021), p. 129656, 10.1016/j.chemosphere.2021.129656
Article
Download PDFView Record in ScopusGoogle Scholar

Henry, 1989
C.D. Henry
Late cenozoic Basin and range structure in western Mexico adjacent to the Gulf of California
GSA Bull., 101 (1989), pp. 1147-1156, 10.1130/0016-7606(1989)101<1147:LCBARS>2.3.CO;2
View Record in ScopusGoogle Scholar

Hooda, 2010
P. Hooda
Trace elements in soils
https://doi.org/10.1002/9781444319477.ch1 (2010)
Google Scholar

INEGI, 2020

INEGI
Censo población y vivienda 2020
[WWW Document], URL
https://www.inegi.org.mx/programas/ccpv/2020/ (2020)
3.5.21
Google Scholar

Jackson et al., 2002
M.L. Jackson, S.A. Tyler, A.L. Willis, G.A. Bourbeau, R.P. Pennington
Weathering sequence of clay-size minerals in soils and sediments
I. Fundamental Generalizations (2002), 10.1021/j150463a015
Google Scholar

Kebonye et al., 2017
N.M. Kebonye, P.N. Eze, F.O. Akinyemi
Long term treated wastewater impacts and source identification of heavy metals in semi-arid soils of Central Botswana
Geoderma Reg., 10 (2017), pp. 200-214, 10.1016/j.geodrs.2017.08.001
Article
Download PDFView Record in ScopusGoogle Scholar

Khodaverdiloo et al., 2020
H. Khodaverdiloo, F.X. Han, R.H. Taghlidabad, A. Karimi, N. Moradi, J.A. Kazery
Potentially toxic element contamination of arid and semi-arid soils and its phytoremediation
Arid Land Res. Manag., 34 (2020), pp. 361-391, 10.1080/15324982.2020.1746707
View Record in ScopusGoogle Scholar

Le Maitre et al., 2002
R.W. Le Maitre, A. Streckeisen, B. Zanettin, M.J. Le Bas, B. Bonin, P. Bateman (Eds.), Igneous Rocks: A Classification and Glossary of Terms: Recommendations of the International Union of Geological Sciences Subcommission on the Systematics of Igneous Rocks (second ed.), Cambridge University Press, Cambridge (2002), 10.1017/CBO9780511535581
Google Scholar

Liu et al., 2018
T. Liu, M.E. Marlier, R.S. DeFries, D.M. Westervelt, K.R. Xia, A.M. Fiore, L.J. Mickley, D.H. Cusworth, G. Milly
Seasonal impact of regional outdoor biomass burning on air pollution in three Indian cities: Delhi, Bengaluru, and Pune
Atmos. Environ., 172 (2018), pp. 83-92, 10.1016/j.atmosenv.2017.10.024
Article
Download PDFView Record in ScopusGoogle Scholar

Liu et al., 2020
Z. Liu, L. Shen, C. Yan, J. Du, Y. Li, H. Zhao
Analysis of the influence of precipitation and wind on PM2.5 and PM10 in the atmosphere
Adv. Meteorol. 2020 (2020), Article e5039613, 10.1155/2020/5039613
Google Scholar

Madhavaraju et al., 2016
J. Madhavaraju, M. Tom, Y.I. Lee, V. Balaram, S. Ramasamy, A. Carranza-Edwards, A. Ramachandran
Provenance and tectonic settings of sands from Puerto Peñasco, desemboque and bahia Kino beaches, Gulf of California, Sonora, México
J. South Am. Earth Sci., 71 (2016), pp. 262-275, 10.1016/j.jsames.2016.08.005

Article
Download PDFView Record in ScopusGoogle Scholar
Mazhaiskii et al., 2000
Y. Mazhaiskii, O. Zakharova, V. Evtyukhin, s.A. Tobratov
Pollution in the zone around ryazan power station
Chem. Pet. Eng. - CHEM Pet. ENG-ENGL TR, 36 (2000), pp. 607-610, 10.1023/A:1002828513234
View Record in ScopusGoogle Scholar
McLennan, 1989
S.M. McLennan
Rare earth elements in sedimentary rocks; influence of provenance and sedimentary processes
Rev. Mineral. Geochem., 21 (1989), pp. 169-200
CrossRefView Record in ScopusGoogle Scholar
McLennan et al., 1993
S.M. McLennan, S. Hemming, D.K. McDaniel, G.N. Hanson
Geochemical approaches to sedimentation, provenance, and tectonics
https://doi.org/10.1130/SPE284-p21 (1993)
Google Scholar
Meza-Figueroa et al., 2007
D. Meza-Figueroa, M. De la O-Villanueva, M.L. De la Parra
Heavy metal distribution in dust from elementary schools in Hermosillo, Sonora, México. Atmos
Environ. Times, 41 (2007), pp. 276-288, 10.1016/j.atmosenv.2006.08.034
Article
Download PDFView Record in ScopusGoogle Scholar
Meza-Figueroa et al., 2016
D. Meza-Figueroa, B. González-Grijalva, R. Del Río-Salas, R. Coimbra, L. Ochoa-Landin, V. Moreno-Rodríguez
Traffic signatures in suspended dust at pedestrian levels in semiarid zones: implications for human exposure
Atmos. Environ., 138 (2016), pp. 4-14, 10.1016/j.atmosenv.2016.05.005
Article
Download PDFView Record in ScopusGoogle Scholar
Meza-Figueroa et al., 2018
D. Meza-Figueroa, B. González-Grijalva, F. Romero, J. Ruiz, M. Pedroza-Montero, C.I.-D. Rivero, M. Acosta-Elías, L. Ochoa-Landin, S. Navarro-Espinoza
Source apportionment and environmental fate of lead chromates in atmospheric dust in arid environments
Sci. Total Environ., 630 (2018), pp. 1596-1607, 10.1016/j.scitotenv.2018.02.285
Article
Download PDFView Record in ScopusGoogle Scholar
Meza-Montenegro et al., 2012
M.M. Meza-Montenegro, A.J. Gandolfi, M.E. Santana-Alcántar, W.T. Klimecki, M.G. Aguilar-Apodaca, R. Del Río-Salas, M. De la O-Villanueva, A. Gómez-Alvarez, H. Mendivil-Quijada, M. Valencia, D. Meza-Figueroa
Metals in residential soils and cumulative risk assessment in Yaqui and Mayo agricultural valleys, northern Mexico
Sci. Total Environ., 433 (2012), pp. 472-481, 10.1016/j.scitotenv.2012.06.083
Article
Download PDFView Record in ScopusGoogle Scholar

Middelburg et al., 1988
J.J. Middelburg, C.H. van der Weijden, J.R.W. Woittiez
Chemical processes affecting the mobility of major, minor and trace elements during weathering of granitic rocks
Chem. Geol., 68 (1988), pp. 253-273, 10.1016/0009-2541(88)90025-3
Article
Download PDFView Record in ScopusGoogle Scholar
Mikkonen et al., 2018
H.G. Mikkonen, R. Dasika, J.A. Drake, C.J. Wallis, B.O. Clarke, S.M. Reichman
Evaluation of environmental and anthropogenic influences on ambient background metal and metalloid concentrations in soil
Sci. Total Environ., 624 (2018), pp. 599-610, 10.1016/j.scitotenv.2017.12.131
Article
Download PDFView Record in ScopusGoogle Scholar
Minasny et al., 2008
B. Minasny, AlexB. McBratney, S. Salvador-Blanes
Quantitative models for pedogenesis — a review
Geoderma, Antarctic Soils and Soil Forming Processes in a Changing Environment, 144 (2008), pp. 140-157, 10.1016/j.geoderma.2007.12.013
Article
Download PDFGoogle Scholar
Moore and Carpi, 2005
C. Moore, A. Carpi
Mechanisms of the emission of mercury from soil: role of UV radiation
J. Geophys. Res. Atmospheres, 110 (2005), 10.1029/2004JD005567
Google Scholar
Moreno et al., 2010
T. Moreno, X. Querol, A. Alastuey, J. de la Rosa, A.M.S. de la Campa, M. Minguillón, M. Pandolfi, Y. González-Castanedo, E. Monfort, W. Gibbons
Variations in vanadium, nickel and lanthanoid element concentrations in urban air
Sci. Total Environ., 408 (2010), pp. 4569-4579
Article
Download PDFView Record in ScopusGoogle Scholar
Moreno et al., 2008
T. Moreno, X. Querol, A. Alastuey, W. Gibbons
Identification of FCC refinery atmospheric pollution events using lanthanoid- and vanadium-bearing aerosols
Atmos. Environ., 42 (2008), pp. 7851-7861, 10.1016/j.atmosenv.2008.07.013
Article
Download PDFView Record in ScopusGoogle Scholar
Moreno-Rodríguez et al., 2015
V. Moreno-Rodríguez, R. Del Rio-Salas, D.K. Adams, L. Ochoa-Landin, J. Zepeda, A. Gómez-Alvarez, J. Palafox-Reyes, D. Meza-Figueroa
Historical trends and sources of TSP in a Sonoran desert city: can the North America Monsoon enhance dust emissions? Atmos
Environ. Times, 110 (2015), pp. 111-121, 10.1016/j.atmosenv.2015.03.049
Article
Download PDFView Record in ScopusGoogle Scholar
Mukherjee et al., 2020
I. Mukherjee, U.K. Singh, R.P. Singh, Anshumali, D. Kumari, P.K. Jha, P. Mehta

Characterization of heavy metal pollution in an anthropogenically and geologically influenced semi-arid region of east India and assessment of ecological and human health risks
Sci. Total Environ., 705 (2020), p. 135801, 10.1016/j.scitotenv.2019.135801
Article
Download PDFView Record in ScopusGoogle Scholar

Murphy, 2000
J. Murphy
Tectonic influence on sedimentation along the southern flank of the late Paleozoic Magdalen basin in the Canadian Appalachians: geochemical and isotopic constraints on the Horton Group in the St. Marys basin
Nova Scotia. Geol. Soc. Am. Bull., 112 (2000), pp. 997-1011, 10.1130/0016-7606(2000)112<997:TIOSAT>2.0.CO;2
Google Scholar

Navarro et al., 2004
A. Navarro, D. Collado, M. Carbonell, J.A. Sanchez
Impact of mining activities on soils in a semi-arid environment: sierra Almagrera district, SE Spain
Environ. Geochem. Health, 26 (2004), pp. 383-393, 10.1007/s10653-005-5361-0
View Record in ScopusGoogle Scholar

Navarro et al., 2008
M.C. Navarro, C. Pérez-Sirvent, M.J. Martínez-Sánchez, J. Vidal, P.J. Tovar, J. Bech
Abandoned mine sites as a source of contamination by heavy metals: a case study in a semi-arid zone
J. Geochem. Explor., Trace elements in soils: Baseline levels and imbalance, 96 (2008), pp. 183-193, 10.1016/j.gexplo.2007.04.011
Article
Download PDFView Record in ScopusGoogle Scholar

Navarro et al., 2007
R. Navarro, J. Guzman, I. Saucedo, J. Revilla, E. Guibal
Vanadium recovery from oil fly ash by leaching, precipitation and solvent extraction processes
Waste Manag., 27 (2007), pp. 425-438, 10.1016/j.wasman.2006.02.002
Article
Download PDFView Record in ScopusGoogle Scholar

Nesbitt et al., 1997
H.W. Nesbitt, C.M. Fedo, G.M. Young
Quartz and feldspar stability, steady and non-steady-state weathering, and petrogenesis of siliciclastic sands and Muds
J. Geol., 105 (1997), pp. 173-192, 10.1086/515908
Google Scholar

Nesbitt and Young, 1984
H.W. Nesbitt, G.M. Young
Prediction of some weathering trends of plutonic and volcanic rocks based on thermodynamic and kinetic considerations
Geochem. Cosmochim. Acta, 48 (1984), pp. 1523-1534, 10.1016/0016-7037(84)90408-3
Article
Download PDFView Record in ScopusGoogle Scholar

Nesbitt and Young, 1982
H.W. Nesbitt, G.M. Young

Early Proterozoic climates and plate motions inferred from major element chemistry of lutites
Nature, 299 (1982), pp. 715-717, 10.1038/299715a0
View Record in ScopusGoogle Scholar

Ochoa-Contreras et al., 2021
R. Ochoa-Contreras, M.E. Jara-Marini, J.-A. Sanchez-Cabeza, D.M. Meza-Figueroa, L.H. Pérez-Bernal, A.C. Ruiz-Fernández
Anthropogenic and climate induced trace element contamination in a water reservoir in northwestern Mexico
Environ. Sci. Pollut. Res. (2021), 10.1007/s11356-020-11995-3
Google Scholar

Olguín-Villa et al., 2013
A.E. Olguín-Villa, J.R. Vidal-Solano, J.M. Stock
Petrografía, geoquímica, petrofábrica y paleomagnetismo de la Toba de San Felipe en la región de Cataviña, Baja California
México. Rev. Mex. Cienc. Geológicas, 30 (2013), pp. 282-298
View Record in ScopusGoogle Scholar

Ortega et al., 2013
B. Ortega, P. Schaaf, A. Murray, M. Caballero, S. Lozano, A. Ramirez
Eolian deposition cycles since AD 500 in playa san bartolo lunette dune, Sonora, Mexico: paleoclimatic implications
Aeolian Res., 11 (2013), pp. 1-13, 10.1016/j.aeolia.2013.06.002
Article
Download PDFView Record in ScopusGoogle Scholar

Ortlieb, 1991
L. Ortlieb
Quaternary shorelines along the Northeastern Gulf of California ; geochronological data and neotectonic implications
Geol. Soc. Am. Spec. Pap., 254 (1991), 10.1130/SPE254-p95
Google Scholar

Paladino et al., 2017
O. Paladino, A. Moranda, M. Seyedsalehi
A method for identifying pollution sources of heavy metals and PAH for a risk-based Management of a Mediterranean harbour
Scientifica 2017 (2017), Article e4690715, 10.1155/2017/4690715
Google Scholar

Pastrana-Corral et al., 2017
M.A. Pastrana-Corral, F.T. Wakida, J. Temores-Peña, D.D. Rodriguez-Mendivil, E. García-Flores, T.D.J. Piñon-Colin, A. Quiñonez-Plaza
Heavy metal pollution in the soil surrounding a thermal power plant in Playas de Rosarito, Mexico
Environ. Earth Sci., 76 (2017), p. 583, 10.1007/s12665-017-6928-7
View Record in ScopusGoogle Scholar

Potter et al., 2005
Overview
P.E. Potter, J.B. Maynard, P.J. Depetris (Eds.), Mud and Mudstones: Introduction and Overview, Springer, Berlin, Heidelberg (2005), pp. 1-6, 10.1007/3-540-27082-5_1
Google Scholar

Pourret and Bollinger, 2018
O. Pourret, J.-C. Bollinger
Heavy metal" - what to do now: to use or not to use?

Sci. Total Environ., 610–611 (2018), pp. 419-420, 10.1016/j.scitotenv.2017.08.043
Article
Download PDFView Record in ScopusGoogle Scholar

Prabhakar et al., 2014
G. Prabhakar, A. Sorooshian, E. Toffol, A.F. Arellano, E.A. Betterton
Spatiotemporal distribution of airborne particulate metals and metalloids in a populated arid region
Atmos. Environ., 92 (2014), pp. 339-347, 10.1016/j.atmosenv.2014.04.044
Article
Download PDFView Record in ScopusGoogle Scholar

R n.d. R Core Team, 2020
R Core Team
R: A Language and Environment for Statistical Computing
R Foundation for Statistical Computing, Vienna, Austria (2020)
https://www.R-project.org/
https://www.eea.europa.eu/data-and-maps/indicators/oxygen-consuming-substances-in-rivers/r-development-core-team-2006
11.20.20, URL [WWW Document]. URL
Google Scholar

Ravankhah et al., 2017
N. Ravankhah, R. Mirzaei, S. Masoum
Determination of heavy metals in surface soils around the brick kilns in an arid region, Iran
J. Geochem. Explor., Potentially Toxic Metals in the Environ., 176 (2017), pp. 91-99, 10.1016/j.gexplo.2016.01.005
Article
Download PDFView Record in ScopusGoogle Scholar

Razo et al., 2004
I. Razo, L. Carrizales, J. Castro, F. Díaz-Barriga, M. Monroy
Arsenic and heavy metal pollution of soil, water and sediments in a semi-arid climate mining area in Mexico. Water
Air. Soil Pollut., 152 (2004), pp. 129-152, 10.1023/B:WATE.0000015350.14520.c1
View Record in ScopusGoogle Scholar

Reimann and de Caritat, 2017
C. Reimann, P. de Caritat
Establishing geochemical background variation and threshold values for 59 elements in Australian surface soil
Sci. Total Environ., 578 (2017), pp. 633-648, 10.1016/j.scitotenv.2016.11.010
Article
Download PDFView Record in ScopusGoogle Scholar

Reimann and Garrett, 2005
C. Reimann, R.G. Garrett
Geochemical background—concept and reality
Sci. Total Environ., 350 (2005), pp. 12-27, 10.1016/j.scitotenv.2005.01.047
Article
Download PDFView Record in ScopusGoogle Scholar

Roser et al., 1996
B.P. Roser, R.A. Cooper, S. Nathan, A.J. Tulloch
Reconnaissance sandstone geochemistry, provenance, and tectonic setting of the lower Paleozoic terranes of the West Coast and Nelson, New Zealand
N. Z. J. Geol. Geophys., 39 (1996), pp. 1-16, 10.1080/00288306.1996.9514690

View Record in ScopusGoogle Scholar
Roser and Korsch, 1986
B.P. Roser, R.J. Korsch
Determination of tectonic setting of sandstone-Mudstone suites using SiO_{2} content and $K_{2}O/Na_{2}O$ ratio
J. Geol., 94 (1986), pp. 635-650
CrossRefView Record in ScopusGoogle Scholar
Rueda-Holgado et al., 2016
F. Rueda-Holgado, L. Calvo-Blázquez, F. Cereceda-Balic, E. Pinilla-Gil
Temporal and spatial variation of trace elements in atmospheric deposition around the industrial area of Puchuncaví-Ventanas (Chile) and its influence on exceedances of lead and cadmium critical loads in soils
Chemosphere, 144 (2016), pp. 1788-1796, 10.1016/j.chemosphere.2015.10.079
Article
Download PDFView Record in ScopusGoogle Scholar
Silva et al., 2018
C. Silva, R. Barbosa, Yuri Silva, Ygor Silva
Spatial variability of rare earth elements in soils under different geological and climate patterns of the Brazilian northeast
Rev. Bras. Ciênc. Solo, 42 (2018), 10.1590/18069657rbcs20170342
Google Scholar
Stock et al., 1999
J.M. Stock, C.J. Lewis, E.A. Nagy
The Tuff of San Felipe: an extensive middle Miocene pyroclastic flow deposit in Baja California, Mexico
J. Volcanol. Geoth. Res., 93 (1999), pp. 53-74, 10.1016/S0377-0273(99)00079-7
Article
Download PDFView Record in ScopusGoogle Scholar
Suttner and Dutta, 1986
L.J. Suttner, P.K. Dutta
Alluvial sandstone composition and paleoclimate; I, Framework mineralogy
J. Sediment. Res., 56 (1986), pp. 329-345, 10.1306/212F8909-2B24-11D7-8648000102C1865D
View Record in ScopusGoogle Scholar
Taboada et al., 2006
T. Taboada, A.M. Cortizas, C. García, E. García-Rodeja
Particle-size fractionation of titanium and zirconium during weathering and pedogenesis of granitic rocks in NW Spain
Geoderma, 131 (2006), pp. 218-236, 10.1016/j.geoderma.2005.03.025
Article
Download PDFView Record in ScopusGoogle Scholar
Thorpe and Harrison, 2008
A. Thorpe, R.M. Harrison
Sources and properties of non-exhaust particulate matter from road traffic: a review
Sci. Total Environ., 400 (2008), pp. 270-282, 10.1016/j.scitotenv.2008.06.007
Article
Download PDFView Record in ScopusGoogle Scholar
Tijhuis et al., 2002
L. Tijhuis, B. Brattli, O. Sæther
A geochemical survey of topsoil in the city of oslo, Norway
Environ. Geochem. Health, 24 (2002), pp. 67-94, 10.1023/A:1013979700212

View Record in ScopusGoogle Scholar
Tripathee et al., 2016
L. Tripathee, S. Kang, D. Rupakheti, Q. Zhang, R.M. Bajracharya, C.M. Sharma, J. Huang, A. Gyawali, R. Paudyal, M. Sillanpää
Spatial distribution, sources and risk assessment of potentially toxic trace elements and rare earth elements in soils of the Langtang Himalaya, Nepal
Environ. Earth Sci., 75 (2016), p. 1332, 10.1007/s12665-016-6140-1
View Record in ScopusGoogle Scholar
Valencia-Moreno et al., 2011
M. Valencia-Moreno, J. Ruiz, L. Ochoa-Landín, R. Martínez-Serrano, P. Vargas-Navarro
Geochemistry of the coastal Sonora batholith, northwestern Mexico
Can. J. Earth Sci. (2011), 10.1139/e03-020
Google Scholar
Velderrain-Rojas et al., 2021
L.A. Velderrain-Rojas, J.R. Vidal-Solano, L.M. Alva-Valdivia, R. Vega-Granillo
Late miocene silicic subvolcanic plumbing system related to oblique rifting in the Pacific-North American plate boundary, Sonora, Mexico: geodynamic implication in a regional context
Int. Geol. Rev. (2021), pp. 1-27, 10.1080/00206814.2021.1878396
0
Google Scholar
Vidal-Solano et al., 2007
J.R. Vidal-Solano, F.A. Paz-Moreno, A. Demant, M. López-Martínez
Ignimbritas hiperalcalinas del Mioceno medio en Sonora Central: revaluación de la estratigrafía y significado del volcanismo terciario
Rev. Mex. Ciencias Geol., 24 (2007), pp. 47-67
View Record in ScopusGoogle Scholar
Wang et al., 2008
X. Wang, J. Huang, M. Ji, K. Higuchi
Variability of East Asia dust events and their long-term trend
Atmos. Environ., 42 (2008), pp. 3156-3165, 10.1016/j.atmosenv.2007.07.046
Article
Download PDFView Record in ScopusGoogle Scholar
Warke, 2013
P. Warke
Weathering in arid regions
Treatise Geomorphol, 4 (2013), pp. 197-227, 10.1016/B978-0-12-374739-6.00060-9
Article
Download PDFView Record in ScopusGoogle Scholar
Weissmannová and Pavlovský, 2017
H.D. Weissmannová, J. Pavlovský
Indices of soil contamination by heavy metals – methodology of calculation for pollution assessment (minireview)
Environ. Monit. Assess., 189 (2017), p. 616, 10.1007/s10661-017-6340-5
View Record in ScopusGoogle Scholar
Xia et al., 2015
D. Xia, Y. Deng, S. Wang, S. Ding, C. Cai
Fractal features of soil particle-size distribution of different weathering profiles of the collapsing gullies in the hilly granitic region, south China
Nat. Hazards, 79 (2015), pp. 455-478, 10.1007/s11069-015-1852-1
View Record in ScopusGoogle Scholar

Yang et al., 2017
L. Yang, G. Zhu, H. Pan, P. Shi, J. Li, Y. Liu, H. Tong
Surface dust heavy metals in the major cities, China
Environ. Earth Sci., 76 (2017), p. 757, 10.1007/s12665-017-7084-9
Google Scholar
Yang and Williams, 2015
X. Yang, M. Williams
Landforms and processes in arid and semi-arid environments
CATENA, Landforms and processes in arid and semi-arid environments, 134 (2015), pp. 1-3, 10.1016/j.catena.2015.02.011
Article
Download PDFGoogle Scholar
Zheng et al., 2016
X. Zheng, X. Guo, W. Zhao, T. Shu, Y. Xin, X. Yan, Q. Xiong, F. Chen, M. Lv
Spatial variation and provenance of atmospheric trace elemental deposition in Beijing
Atmospheric Pollut. Res., 7 (2016), pp. 260-267, 10.1016/j.apr.2015.10.006
Article
Download PDFView Record in ScopusGoogle Scholar